

Interaction of the potent antitumoral compounds Casiopeinas® with blood serum and cellular bioligands

Valeria Ugone^a, Federico Pisanu^b, Daniele Sanna^{a,*}, Eugenio Garribba^{b,*}

^a Istituto CNR di Chimica Biomolecolare, Trav. La Crucca 3, I-07100 Sassari, Italy

^b Dipartimento di Chimica e Farmacia, Università di Sassari, Via Vienna 2, I-07100 Sassari, Italy

* Corresponding authors.

E-mail addresses: daniele.sanna@cnr.it (D. Sanna); garribba@uniss.it (E. Garribba).

Abstract

Casiopeinas® are among the few Cu^{II} compounds patented for their antitumor activity, but their mode of action has not been fully elucidated yet. One of them, Cas II-gly, is formed by 4,7-dimethyl-1,10-phenanthroline (Me₂phen) and glycinato (Gly). In blood and cells, Cas II-gly can keep its identity or form mixed species with serum or cytosol bioligands (*bL* or *cL*) with composition Cu^{II}-Me₂phen-*bL/cL*, Cu^{II}-Gly-*bL/cL*, or Cu^{II}-*bL/cL*. In this study, the binding of Cas II-gly with low molecular mass bioligands of blood serum (citric, L-lactic acid, and L-histidine) and cytosol (reduced glutathione (GSH), reduced nicotinamide adenine dinucleotide (NADH), adenosine triphosphate (ATP), and L-ascorbic acid) was examined through the application of instrumental (ElectroSpray Ionization-Mass Spectrometry and Electron Paramagnetic Resonance) and computational (Density Functional Theory) methods. The results indicated that mixed species Cu^{II}-Me₂phen-*bL/cL* are formed, with the bioligands replacing glycinato. The formation of these adducts may participate in the copper transport toward the target organs and facilitate the cellular uptake or, in contrast, preclude it. In the systems with GSH, NADH and L-ascorbate, a redox reaction occurs with the partial oxidation of *cL* to the corresponding oxidized form (GSSG, NAD⁺ and dehydroascorbate) which interact with Cu^{II}. Formed Cu^I ion does not give complexation reactions with reduced or oxidized form of bioligands for its 'soft' character and low affinity for oxygen and nitrogen donors compared to Cu^{II}. However, Cu^I could promote Fenton-like reactions with production of reactive oxygen species (ROS) related to the antitumor activity of Casiopeinas®.

Keywords

Copper, antitumor compounds, serum bioligands, cellular bioligands, transport, active species

1. Introduction

Copper (Cu) is an essential element for all living systems, with a fundamental role – among others – for cellular respiration, heme synthesis and iron uptake. Cu-proteins transport oxygen in invertebrate organisms and participate in electron transfer, redox processes, and oxygenation reactions of organic substrates [1-4]. The stability of its two oxidation states (+I and +II) accounts for its catalytic and electron exchange role. Defects in Cu absorption and transport are related to Menkes syndrome and Wilson's disease [5].

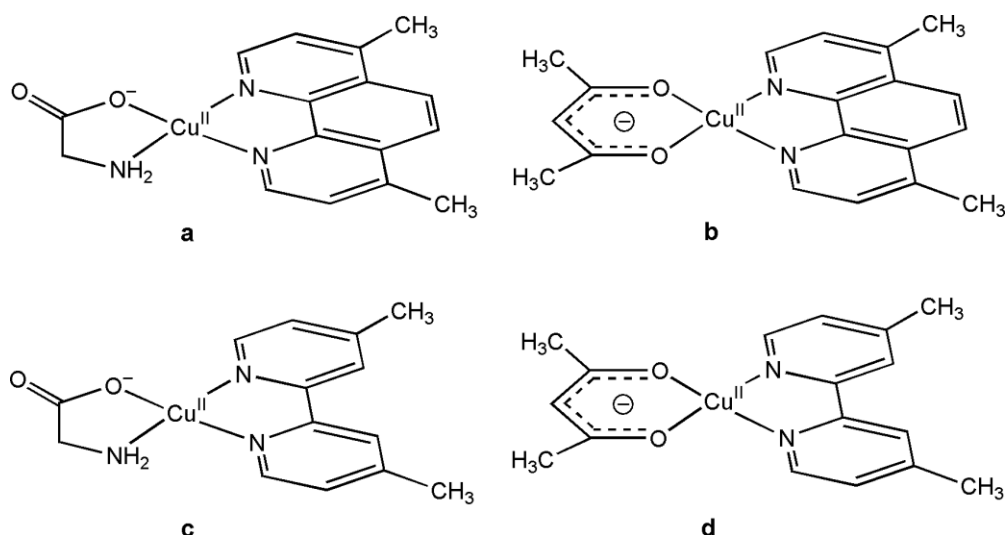
In the recent years, the interest for Cu coordination compounds as potential drugs has increased exponentially and many reviews have been published on this topic [6-11]. Based on the assumption that copper, an endogenous metal, may be less toxic than other metals, like platinum, various Cu complexes have been proposed as anticancer agents to replace or integrate the use of cisplatin; in fact, the latter – although effective against several types of cancer – has many limitations, such as side effects and resistance phenomena due to the prolonged administration [10, 12]. Some *in vivo* studies have shown that the concentration of copper in cancer cells is higher than in healthy cells and an increase in the Cu concentration is also observed in blood serum of cancer patients [10]. The reasons of this increase have not yet been defined, but it was hypothesized that this is related to the role of copper as a stimulator of angiogenesis, i.e., the development of new blood vessels from the existing ones, necessary for the proliferation of the tumor mass [13]. Other studies have shown that high concentrations of copper inside the cells block the action of some inhibitors of apoptosis, such as proteins known as X-linked inhibitor of apoptosis (XIAP), promoting the cell death [14].

The first pioneering studies on the copper-based anticancer drugs started from these two experimental evidences. The higher amount of Cu in cancer than in healthy cells suggested that the cancer cells could be the target of the drug [10]. Therefore, if an organic ligand exhibits antitumor activity in the free form, its administration coordinated to copper could facilitate the uptake by cancer cells. The mechanism of action of pharmacologically active Cu compounds is not yet fully understood; the most accepted hypothesis is based on the intracellular formation of reactive oxygen species (ROS) through thiol-mediated reduction from Cu^{II} to Cu^I and the subsequent Fenton-like reaction between the Cu^I ion and H₂O₂ [15, 16]. The reduction mechanism in the cellular environment remains unclear, but it is assumed that Cu^{II} is reduced by (a) thiol compound(s), such as cysteine, glutathione, or transport proteins [17].

Up to now, few copper compounds were patented. Among them, the family of Casiopeinas® is worth being mentioned. Casiopeinas® comprise a series of Cu^{II} complexes with general formula [Cu^{II}(L^{N-N})(L^{N-O})]NO₃ and [Cu^{II}(L^{N-N})(L^{O-O})]NO₃, where L^{N-N} is a heterocyclic aromatic ligand such as 1,10-phenanthroline (phen) or 2,2'-bipyridine (bipy) and substituted analogs (i.e. 4,7-

dimethyl-1,10-phenanthroline (Me₂phen) or 4,4'-dimethyl-2,2'-bipyridine (Me₂bipy)), and L^{N-O} and L^{O-O} are monoanions derived from an amino acid, acetylacetonate, or salicylaldehyde [18]. Casiopeinas® have been fully characterized by analytical methods and their structure has been resolved by X-ray diffraction [19-21]. Chemical and structural data show that the geometry around the copper(II) ion is variable and ranges, in the solid state, from square planar to square pyramidal and distorted octahedral with the presence of the counterion or water molecules in the axial positions. In the 90s of the last century, Casiopeinas® were registered and patented [22-24]. Their extensive aromatic ring system allows these species to bind to DNA by intercalative and non-intercalative mode either as free ligands or metal complexes [25, 26]. Amino acids and acetylacetonate were chosen for their low toxicity and for thermodynamic stability of the mixed species formed with Cu(bipy)²⁺ and Cu(phen)²⁺ moieties [27, 28], as well as to modulate the redox properties of the metal center. The analysis of the structure-activity relationships suggested that the nature, number, and position of the substituents on heterocyclic ligands and the identity of the amino acid have a crucial effect on the selectivity or degree of biological activity exhibited by these species [18]. These findings were related to the change in some physico-chemical properties of the complexes, such as the redox behavior of the copper center or their solubility in water [29].

Casiopeinas® have been tested on various cancer cell lines, including HeLa, SiHa, MCF-7, and HCT-15. The found IC₅₀ values were, generally, below 50 μM; for example, [Cu^{II}(Me₂phen)(acac)]NO₃ (named Cas III-Ea) showed values of 10.7±0.9 μM, 6.8±0.9 μM, 8.1±0.5 μM and 7.3±0.7 μM, respectively [18]. Among the Casiopeinas® with higher pharmacological activity are worth of being mentioned Cas II-gly, Cas III-Ea, Cas IV-gly and Cas III-ia, in which the Cu^{II} ion is bound by a Me₂phen or Me₂bipy molecule and a glycinate or acetylacetonate anion with nitrate acting as a counterion (Scheme 1).



Scheme 1. Structure of some Cu^{II} complexes belonging to Casiopeinas® family: (a) [Cu^{II}(Me₂phen)(Gly)]⁺ (Cas II-gly), (b) [Cu^{II}(Me₂phen)(acac)]⁺ (Cas III-Ea), (c) [Cu^{II}(Me₂bipy)(Gly)]⁺ (Cas IV-gly), and (d) [Cu^{II}(Me₂bipy)(acac)]⁺ (Cas III-ia). The water molecules eventually bound to the metal ion and NO₃⁻ ion have been omitted for simplicity.

The mode of action of Casiopeinas® has not been fully elucidated and remains the subject of numerous studies, although experimental evidence suggest that these compounds may act with at least three different modes of action: (i) generation of ROS, (ii) mitochondrial toxicity, and (iii) direct interaction with DNA [18]. Casiopeinas II-gly and III-ia inhibit a number of enzymes important for normal mitochondrial function and – in addition – uncouple respiration processes, but the former compound is 10-fold more potent than the latter [30].

When a metallodrug is administered, it follows a path from the site of administration to the site of action before it exerts its pharmacological activity. The different steps can be divided into absorption (if the drug is administered orally) and transport, which is the journey through the circulatory system to the target organ(s), i.e. the tissue(s) or cell(s) where the drug acts. In the bloodstream, the metallodrug becomes a serum solute and it encounters several potential bioligands with high molecular mass such as albumin, transferrin and ceruloplasmin, and low mass like amino acids, citrate, lactate, organic and inorganic phosphates, which may displace the metal-coordinated ligand(s), forming ternary compounds or generating the corresponding binary complexes. Considering the kinetically labile nature of copper complexes [10], ligand exchange reactions (transchelation) are expected that could be strongly favored. These processes result in the formation of mixed species that could be of high importance in the biological and pharmacological activity. Studies of Casiopeinas® transport suggested that substitution of L^{N-N} ligand and L^{N-O} or L^{O-O} coligand can alter their biological activity [31, 32]. Recently, Costa-Pessoa and coworkers

demonstrated that Casiopeinas® can bind to human albumin (HSA), generating a series of adducts in aqueous solution such as Cu^{II} -HSA, $[\text{Cu}^{\text{II}}(\text{Me}_2\text{phen})]$ -HSA, and $[\text{Cu}^{\text{II}}(\text{Me}_2\text{phen})(\text{Gly})]$ -HSA [33].

In this study, the binding of Cas II-gly with low molecular mass (Imm) bioligands of blood serum (*bL*) and cytosol (*cL*) was studied through the combined application of instrumental (ElectroSpray Ionization-Mass Spectrometry (ESI-MS) and Electron Paramagnetic Resonance (EPR)) computational (Density Functional Theory (DFT)) methods. Equimolar amounts of Cas II-gly and *bL/cL* were used in the present study to evaluate the relative strength toward Cu^{II} of Me_2phen , Gly⁻ and serum and cell bioligands. Among the ligands of the serum, citric acid (*citr*; 99.0 μM [34]), L-lactic acid (*lact*; 1.51 mM [34]), and L-histidine (*His*; 77.0 μM [34]) were chosen, while for cellular *cL* reduced glutathione (*GSH*, γ -L-glutamyl-L-cysteinylglycine; 2.23 mM in the erythrocyte cytosol [35]), L-ascorbic acid (*Asc*; 28.9 μM in the erythrocyte cytosol [35]), reduced nicotinamide adenine dinucleotide (*NADH*; 1.8 μM in the erythrocyte cytosol [35]), adenosine triphosphate (*ATP*; 1.35 mM in the erythrocyte cytosol [35]) were examined [36]. The results could provide new information on the importance of the biotransformation processes of this promising class of antitumoral drugs with the aim to modulate their chemical features to improve their effectiveness. In the future, we plan to investigate these systems considering the relative concentration of *bL/cL* under physiological conditions and in real serum samples and the binding of Cas II-gly to proteins.

2. Experimental and computational details

2.1. Materials

Water was deionized prior to use through the purification system Millipore Milli-Q Academic for EPR or purchased from Sigma-Aldrich (LC-MS grade) for ESI-MS. Glycine (Gly) was purchased from Merck (code 4201), 4,7-dimethyl-1,10-phenanthroline from Sigma-Aldrich (code 00615KW), citric acid from Fluka (code 27490) L-lactic acid from Sigma (code L1750), L-histidine from J. T. Baker (code 1603), reduced glutathione from Sigma-Aldrich (code G4251), reduced β -nicotinamide adenine dinucleotide disodium salt hydrate from TCI (code D0920), adenosine 5'-triphosphate disodium salt hydrate from SERVA (code 10920), L-ascorbic acid from Honeywell Riedel-de Haen (code 33034), and $(\text{NH}_4)_2\text{CO}_3$ from Carlo Erba (code 419237).

For EPR measurements, $^{63}\text{CuSO}_4 \cdot 5\text{H}_2\text{O}$ was synthesized from metallic ^{63}Cu with an isotopic purity of 99.9% purchased from Cambridge Isotope Laboratories, Inc., while for ESI-MS CuCl_2 from

Sigma-Aldrich (code 222011) was used. H₂SO₄ (96% v/v), HNO₃ (65% v/v) and HCl (37% v/v), and NaOH as pellets all purchased from Carlo Erba, were also employed.

2.2. EPR measurements

Solutions for EPR were prepared as follows. The molar ratio in the ternary and quaternary systems was 1/1/1 and 1/1/1/1, obtained by mixing appropriate aliquots of aqueous solutions of each individual component (2.5 or 5.0×10^{-3} M) to reach a final Cu^{II} concentration of 1.0×10^{-3} M. The pH values of the solution were varied with diluted solution of H₂SO₄ and NaOH. The spectra were recorded from pH 3 to 9, paying particular attention that at least one was in the pH range 7.2-7.6, i.e. close to the physiological pH. To freeze uniformly the solutions and prevent a concentration gradient during freezing, ethylene glycol was added to each sample.

EPR spectra were recorded immediately after the preparation of the solutions at 120 K with an X-band Bruker EMX spectrometer equipped with a HP 53150A microwave frequency counter and a variable temperature unit. The microwave frequency was 9.40-9.41 GHz, microwave power was 20 mW (which is, with the ER4119 HS resonator, below the saturation limit), time constant was 81.92 ms, modulation frequency 100 kHz, modulation amplitude 0.4 mT, resolution 4096 points.

2.3. ESI-MS measurements

Each solution for ESI-MS measurements was prepared in ultrapure water (LC-MS grade, Sigma-Aldrich) with an equimolar concentration of the components equal to 1.0×10^{-3} M, as described for EPR measurements in section 2.2. The initial pH of each system, in the range 2-3, was brought as close as possible to the neutral value, generally between 6.5 and 7.0 with (NH₄)₂CO₃. Subsequently, the solutions were diluted to 50 μM to record the mass spectra. In the systems with the reductants (*GSH*, *NADH*, and *Asc*), argon was bubbled through the solutions to ensure the absence of oxygen and avoid the oxidation of *cL* by molecular O₂.

Positive- and negative-ion mode ESI-MS spectra were recorded with a high-resolution Q Exactive™ Plus Hybrid Quadrupole-Orbitrap™ mass spectrometer (Thermo Fisher Scientific). The solutions were infused at a flow rate of 5.00 μL/min into the ESI chamber. Spectra were recorded in the range of *m/z* 50-1000 with a resolution of 140000. The instrumental conditions were as follows. Positive-ion mode: spray voltage 2300 V, capillary temperature 250 °C, sheath gas 5-10 (arbitrary units), auxiliary gas 3 (arbitrary units), sweep gas 0 (arbitrary units), probe heater temperature 50 °C. Negative-ion mode: spray voltage -1900 V, capillary temperature 250 °C, sheath gas 20 (arbitrary units), auxiliary gas 5 (arbitrary units), sweep gas 0 (arbitrary units), probe heater temperature 14 °C.

MS/MS spectra were recorded using Normal Collision Energy (NCE) setting in the range of 10-40 and a m/z range of 1.0 around the peak under investigation. Ion fragments were detected at a resolution of 17500. All the mass spectra were analyzed by using Thermo Xcalibur 3.0.63 software (Thermo Fisher Scientific).

2.4. Density functional theory (DFT) calculations

All structures were optimized in the gas phase with Gaussian 09 software (revision *D.01*) [37] at DFT theory level. The hybrid Becke three-parameters B3LYP functional [38, 39] was used combined with the split-valence Pople basis set 6-31g(d,p) for the main group elements, while Stuttgart-Dresden (SDD) implemented with f -functions and pseudo-potential was applied for Cu. These conditions have been successfully applied and discussed in the literature for the geometry prediction of first-row transition metal complexes [40, 41]. Geometry optimizations were carried out without any constraints and minima were verified through frequency calculations. The relative stability of the species in solution was computed at the level of theory B3P86/6-311g(d,p) using the SMD model [42] for the solvent (water) which gives good results in the prediction of Gibbs energy. The Gibbs energy in aqueous solution (G_{aq}) for each species can be separated into the electronic plus nuclear repulsion energy (E_{ele}), the thermal contribution (G_{therm}) and the solvation energy (ΔG_{solv}): $G_{\text{aq}} = E_{\text{ele}} + G_{\text{therm}} + \Delta G_{\text{solv}}$. The term $RT\ln(24.46)$ was considered to account for the standard state correction from the gas phase to the aqueous solution. The thermal contribution was estimated using the ideal gas model and the calculated harmonic vibrational frequencies to determine the correction due to the zero-point energy and thermal population of the vibrational levels.

The ORCA program [43] was used to calculate \mathbf{g} and $\mathbf{A}({}^{63}\text{Cu})$ tensors for some mixed Cu^{II} complexes using the method developed and implemented into the package. The functionals PBE0 [44, 45] and B3LYP [38, 39] with the basis set 6-311g(d,p) was employed to calculate \mathbf{g} and $\mathbf{A}({}^{63}\text{Cu})$, respectively, following the protocol in the literature [46]. Concerning the algebraic signs of the ${}^{63}\text{Cu}$ hyperfine coupling constants, they are negative but their absolute value is reported in this study.

The exchange coupling constant J for $[(\text{Cu}^{\text{II}})_2(\text{Me}_2\text{phen})_2(\text{GSSG})]$, where GSSG is the oxidized form of glutathione, was calculated at the level of theory B3LYP/6-311g with ORCA, using the Heisenberg Hamiltonian $\hat{H} = -J\hat{S}_1 \cdot \hat{S}_2$, where S_1 and S_2 are the spins on two copper atoms [47]. When $S_1 = S_2$, J can be obtained by the expression $J = E_{\text{LS}} - E_{\text{HS}}$, with E_{LS} and E_{HS} energies of the

singlet and triplet state; the energy of the low spin state, E_{LS} , can be determined the broken-symmetry solution, E_{BS} [48].

3. Discussion and results

3.1. Ternary system $Cu^{II}/Me_2phen/Gly$

ESI-MS spectra of the ternary system $Cu^{II}/Me_2phen/Gly$ at 1/1/1 molar ratio were recorded to explore the behavior of Cas II-gly in aqueous solution. The experimental and calculated m/z values of the major species identified in this system are summarized in Table 1. In particular, the spectrum recorded in positive-ion mode shows the presence of signals related to the species $[Cu^{II}(Me_2phen)(Gly)]^+$, with a m/z value of 345.05, $[Cu^{II}(Me_2phen)(H_2O)_2]^{2+}$ (m/z 153.52) $[Cu^I(Me_2phen)]^+$ (m/z 271.03) and $[Cu^{II}(Me_2phen)(OH)]^{2+}$ (m/z 288.03) (Fig. 1). The detection of a Cu^I complex is probably due to the partial reduction of Cu^{II} species in the source, in agreement with the data in the literature [49].

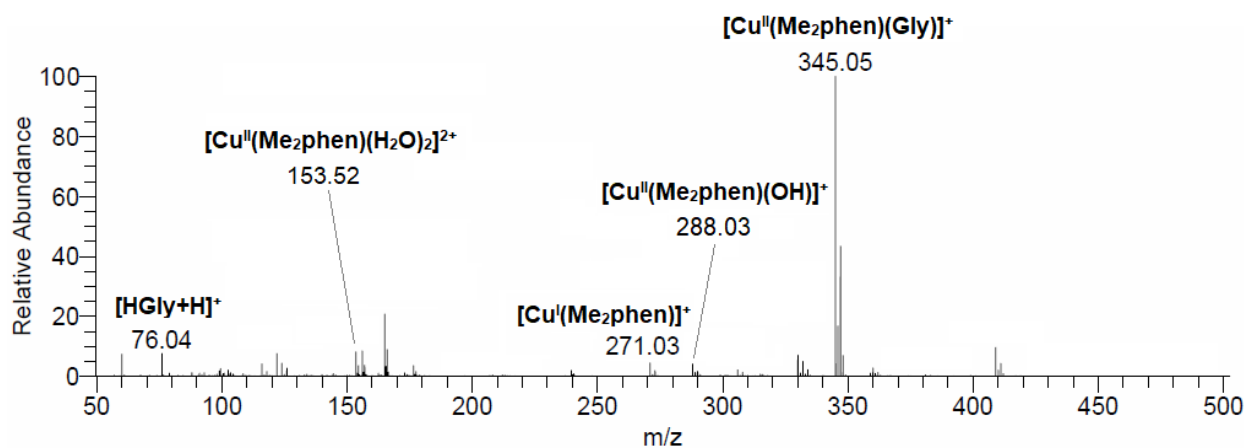


Fig. 1. ESI-MS(+) spectrum recorded on the $Cu^{II}/Me_2phen/Gly$ 1/1/1 system (LC-MS H_2O , Cu^{II} concentration 50 μM).

Table 1. Species identified in the ESI-MS spectra of the system $Cu^{II}/Me_2phen/Gly$.

Species	Composition	m/z (exptl) ^a	m/z (calcd) ^a	Deviation (ppm) ^b
$[Gly+2H]^+$	$C_2H_6NO_2$	76.03932	76.03930	0.3
$[Gly+H+Na]^+$	$C_2H_5NNaO_2$	98.02129	98.02125	0.4
$[Cu^{II}(Me_2phen)]^{2+}$	$C_{14}H_{12}CuN_2$	135.51414	135.51428	-1.0

$[\text{Cu}^{\text{II}}(\text{Me}_2\text{phen})(\text{H}_2\text{O})_2]^{2+}$	$\text{C}_{14}\text{H}_{16}\text{CuN}_2\text{O}_2$	153.52490	153.52484	0.4
$[\text{Cu}^{\text{I}}(\text{Me}_2\text{phen})]^+$	$\text{C}_{14}\text{H}_{12}\text{CuN}_2$	271.02829	271.02910	-3.0
$[\text{Cu}^{\text{I}}(\text{Me}_2\text{phen})(\text{H}_2\text{O})]^+$	$\text{C}_{14}\text{H}_{14}\text{CuN}_2\text{O}$	289.03976	289.03967	0.3
$[\text{Cu}^{\text{II}}(\text{Me}_2\text{phen})(\text{OH})]^+$	$\text{C}_{14}\text{H}_{13}\text{CuN}_2\text{O}$	288.03196	288.03184	0.4
$[\text{Cu}^{\text{II}}(\text{Me}_2\text{phen})(\text{Gly})]^+$	$\text{C}_{16}\text{H}_{16}\text{CuN}_3\text{O}_2$	345.05356	345.05330	0.8

^a Experimental and calculated m/z values refer to the monoisotopic peak with the highest intensity. ^b Error in ppm with respect to the experimental value, calculated as $10^6 \times [\text{Experimental (m/z)} - \text{Calculated (m/z)}] / \text{Calculated (m/z)}$.

As an example, Fig. S1 of the Supporting Information (SI) shows the comparison between the experimental and calculated isotopic pattern of the peak of $[\text{Cu}^{\text{II}}(\text{Me}_2\text{phen})(\text{Gly})]^+$. The pattern is characteristic of natural copper and allows the unambiguous identification of the formed adducts. In particular, the first and most intense peak at m/z 345.05 is due to the isotope ^{63}Cu with natural abundance of 69.1%, while the peak at m/z 347.05 is due to ^{65}Cu which has an abundance of 30.9%. The two intermediate peaks at m/z 346.06 and 348.05 are due to the presence of ^{13}C isotope.

The MS/MS spectrum of the peak related to the mixed species $[\text{Cu}^{\text{II}}(\text{Me}_2\text{phen})(\text{Gly})]^+$ (Fig. 2) shows the presence of the moiety $[\text{Cu}^{\text{I}}(\text{Me}_2\text{phen})]^+$ (m/z = 271.03), generated by the loss of glycine and reduction of copper(II) to copper(I), and $[\text{Cu}^{\text{I}}(\text{Me}_2\text{phen})(\text{H}_2\text{O})]^+$ (m/z = 289.04), a variant of the previous fragment in which a water molecule is bound to copper.

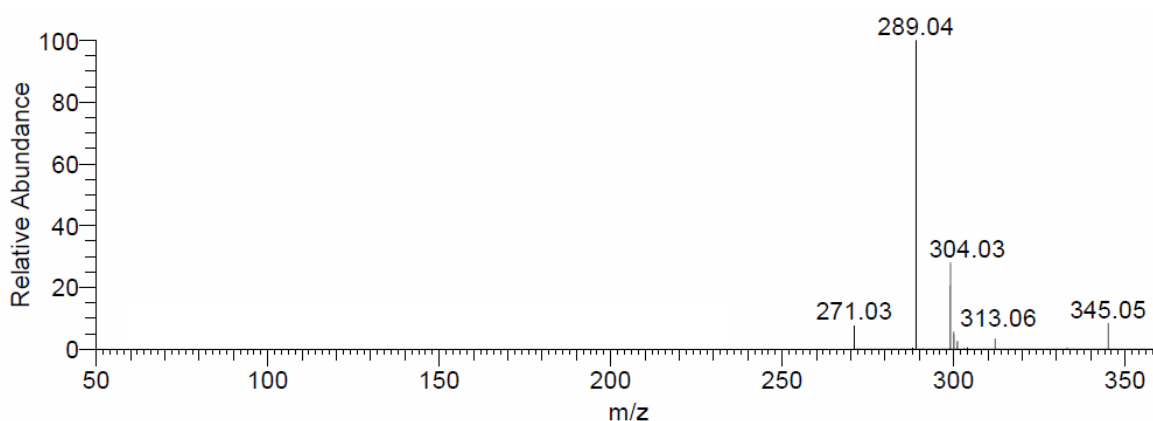


Fig. 2. ESI-MS/MS(+) spectrum of the signal relative to the $[\text{Cu}^{\text{II}}(\text{Me}_2\text{phen})(\text{Gly})]^+$ ion, revealed in the spectra of the $\text{Cu}^{\text{II}}/\text{Me}_2\text{phen}/\text{Gly}$ 1/1/1 system (LC-MS H_2O , Cu^{II} concentration 50 μM), selected in the range of $m/z = 345.05 \pm 0.5$, NCE = 10.

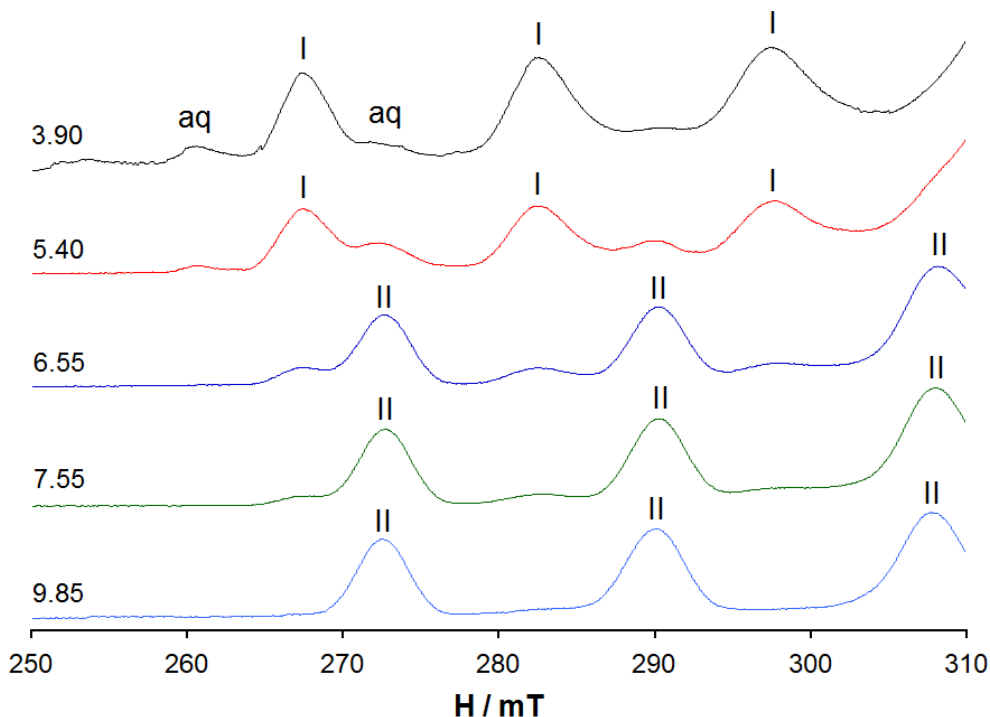


Fig. 3. Low-field region of anisotropic X-band EPR spectra recorded as a function of pH on frozen (120 K) solutions containing $^{63}\text{Cu}^{\text{II}}/\text{Me}_2\text{phen}/\text{Gly}$ 1/1/1 ($^{63}\text{Cu}^{\text{II}}$ concentration 1.0×10^{-3} M). The symbols **aq**, **I** and **II** denote the parallel resonances of aquaion $[\text{Cu}^{\text{II}}(\text{H}_2\text{O})_6]^{2+}$, $[\text{Cu}^{\text{II}}(\text{Me}_2\text{phen})(\text{H}_2\text{O})_4]^{2+}$ and $[\text{Cu}^{\text{II}}(\text{Me}_2\text{phen})(\text{Gly})]^+$.

EPR spectra were recorded on the same ternary system using the ^{63}Cu isotope, which allows for easier detection of the presence of various species in solution and eventual determination of the number of nitrogen atoms coordinated to the metal through superhyperfine coupling. The spectra show that at acid pH only Me_2phen coordinates the metal forming $[\text{Cu}^{\text{II}}(\text{Me}_2\text{phen})(\text{H}_2\text{O})_x]^{2+}$, where $x = 2$ or 4 is the number of water molecules bound to copper, distinguished by $g_z = 2.311$ and $A_z(^{63}\text{Cu}) = 165.5 \times 10^{-4} \text{ cm}^{-1}$, values comparable with those reported in the literature for the analogous 1,10-phenanthroline complex [50]; the first three resonances of the parallel component are indicated by **I** in Fig. 3. The spin-Hamiltonian EPR parameters were calculated with DFT protocol recently validated on fourteen Cu^{II} complexes that allows predicting $A_z(^{63}\text{Cu})$ with B3LYP functional with a mean absolute percent deviation (MAPD) of 8.6% from the experimental value and g_z with PBE0 with a MAPD of 2.9% [46]; it must be noticed that g_z and $A_z(^{63}\text{Cu})$ are the parameters most sensitive to the variation of copper coordination environment and are usually taken into account to hypothesize the coordination mode of a specific complex [51]. The data are listed in Table 2, where emerges that the most plausible hypothesis for $\text{Cu}^{\text{II}}\text{-Me}_2\text{phen}$ species is $[\text{Cu}^{\text{II}}(\text{Me}_2\text{phen})(\text{H}_2\text{O})_4]^{2+}$; the percent deviation (PD) from the experimental g_z is -1.6%, while A_z is

overestimated with PD of 2.6%. These predictions are in line with the previous results in the literature [46, 52].

Table 2. Experimental (exptl) and calculated (calcd) spin Hamiltonian parameters for binary and ternary Cu^{II} complexes.^a

Species	g_z^{exptl}	g_z^{calcd}	PD(g_z) ^b	$A_z(^{63}\text{Cu})^{\text{exptl c}}$	$A_z(^{63}\text{Cu})^{\text{calcd c}}$	PD(A_z) ^b
[Cu ^{II} (Me ₂ phen)(H ₂ O) ₄] ²⁺	2.311	2.273	-1.6	165.5	169.8	2.6
[Cu ^{II} (Me ₂ phen)(H ₂ O) ₂] ²⁺	2.311	2.176	-5.8	165.5	209.2	26.4
[Cu ^{II} (Me ₂ phen)(Gly)] ⁺	2.245	2.218	-1.2	182.8	191.8	4.9
[Cu ^{II} (Me ₂ phen)(<i>citr</i>)] ⁻	2.295	2.257	-1.7	169.1	172.7	2.1
[Cu ^{II} (Me ₂ phen)(<i>lact</i>)] ⁺	2.276	2.230	-2.0	179.1	175.7	-1.9
[Cu ^{II} (Me ₂ phen)(<i>lact</i> H ₋₁)]	2.245	2.201	-2.0	184.3	196.6	6.7
[Cu ^{II} (Me ₂ phen)(<i>His</i>)] ⁺	2.244	2.214	-1.3	184.8	198.0	7.1
[Cu ^{II} (Me ₂ phen) ₂ (H _x ATP)] ^(x-2)	2.291	2.228	-2.7	169.9	181.3	6.7

^a Values of g_z and A_z calculated by DFT methods at the level of theory PBE0/6-311g(d,p) and B3LYP/6-311g(d,p), respectively. ^b Percent deviation of the DFT calculated parameter from the experimental value. ^c Hyperfine coupling constant reported in 10^{-4} cm^{-1} units.

With increasing pH, the deprotonation of the ammonium group of glycinato ligand occurs and the mixed complex [Cu^{II}(Me₂phen)(Gly)]⁺ is formed (**II** in Fig. 3) with $g_z = 2.245$ and $A_z = 182.8 \times 10^{-4} \text{ cm}^{-1}$. The latter is the predominant species in solution around the physiological pH, in agreement with ESI-MS data.

The structure of [Cu^{II}(Me₂phen)(Gly)]⁺ is depicted in Scheme 2a. For this species too, we cannot rule out the presence of one or two water molecules in the axial position(s) to give a square pyramidal or elongated octahedral geometry, also considering that the structure of Cas II-gly in the solid state is hexa-coordinated with an apical water ligand and a nitrate ion [21, 53]. To investigate which species exists in aqueous solution, DFT calculations were performed on the square planar complex and the corresponding solvent-coordinated structure of Cas II-gly. As a starting point, the octahedral X-ray structure of the solid complex [Cu^{II}(Me₂phen)(Gly)(ONO₂)(H₂O)] was taken into account [21, 53]. The variation of the Gibbs energy in aqueous solution, ΔG_{aq} , for the reactions 1 and 2 was computed using the SMD model and the results suggest that the equilibrium is always shifted toward the square planar species with large negative values of ΔG_{aq} (-14.6 kcal/mol for reaction (1) and -9.4 kcal/mol for (2)). The DFT optimized structure of the three Cu^{II} species is shown in Fig. 4.

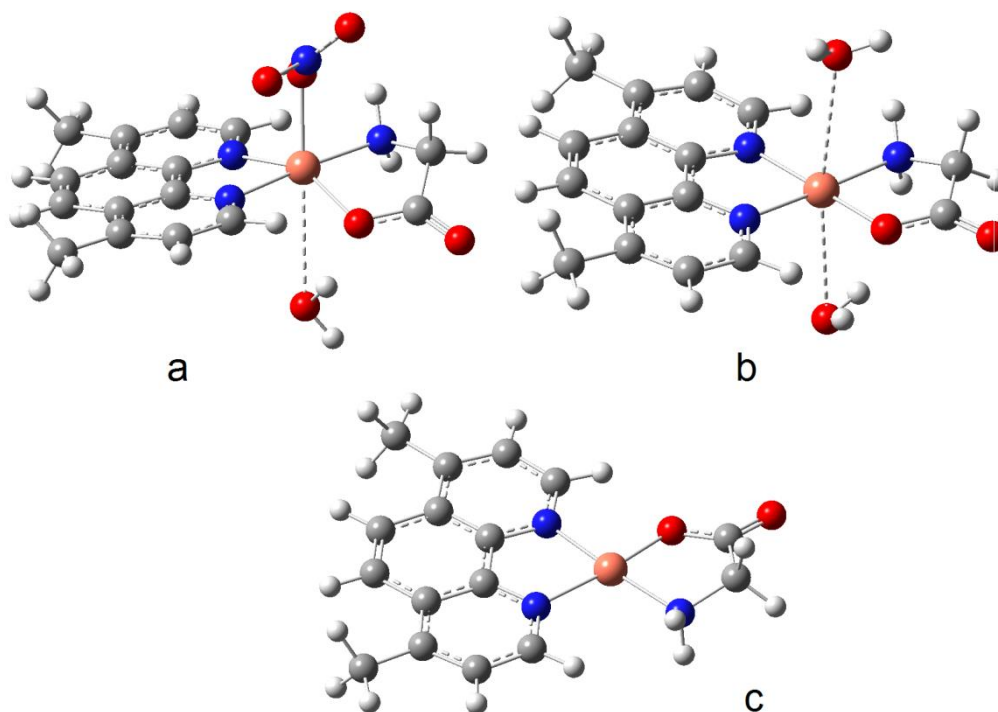
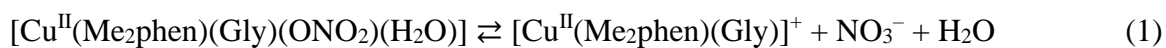


Fig. 4. DFT optimized structures of: a) $[\text{Cu}^{\text{II}}(\text{Me}_2\text{phen})(\text{Gly})(\text{ONO}_2)(\text{H}_2\text{O})]$; b) $[\text{Cu}^{\text{II}}(\text{Me}_2\text{phen})(\text{Gly})(\text{H}_2\text{O})_2]^+$; c) $[\text{Cu}^{\text{II}}(\text{Me}_2\text{phen})(\text{Gly})]^+$.

These data indicate that in solution only the square planar $[\text{Cu}^{\text{II}}(\text{Me}_2\text{phen})(\text{Gly})]^+$ complex should exist.

3.2. Binding to serum bioligands

For a potential metallodrug, the study of the interaction with serum bioligands, for example Imm *bL* and proteins, is essential to ascertain its possible biotransformation and transport of the active species in blood up to the target cells [17, 54-56]. Among the serum bioligands, citrate, lactate, and amino acids, especially His [17], may interact with $\text{Cu}^{\text{II}}\text{-L}$ drugs to form ternary $\text{Cu}^{\text{II}}\text{-L-bL}$ species or the corresponding binary complexes $\text{Cu}^{\text{II}}\text{-bL}$. The formation of such adducts can contribute to the uptake by cells and general action of the metallodrugs. The importance of mixed species around the physiological concentration has been proved for pharmacologically active vanadium compounds such as Metvan [57].

3.2.1. Interaction with citrate

In the ESI-MS spectrum of the $\text{Cu}^{\text{II}}/\text{Me}_2\text{phen}/\text{Gly}/\text{citr}$ 1/1/1 system, citrate-containing species were identified in addition to the complexes already observed in the system with Cas II-gly: the mixed complex $[\text{Cu}^{\text{II}}(\text{Me}_2\text{phen})(\text{citr})+2\text{H}]^+$ ($m/z = 462.05$, Fig. 5) and $[\text{Cu}^{\text{II}}(\text{Me}_2\text{phen})(\text{citr})+\text{H}+\text{Na}]^+$ ($m/z = 484.03$), plus a dinuclear species with stoichiometry $[(\text{Cu}^{\text{II}})_2(\text{Me}_2\text{phen})_2(\text{citr})+\text{H}]^{2+}$ ($m/z = 366.03$), whose concentration in solution is so low that it cannot be detected by EPR spectroscopy (see below). Furthermore, in the spectrum recorded in negative-ion mode, the binary species $[(\text{Cu}^{\text{II}})_2(\text{citr})_2]^{2-}$ ($m/z = 251.93$) was identified. In the dimers, citrate could behave as a bridge between two Cu^{II} ions [58]. The mixed complexes $\text{Cu}^{\text{II}}\text{-Me}_2\text{phen-bL}$ observed by ESI-MS are reported in Table 3, while all the species detected in the quaternary system with Cas II-gly and citrate are listed in Table S1.

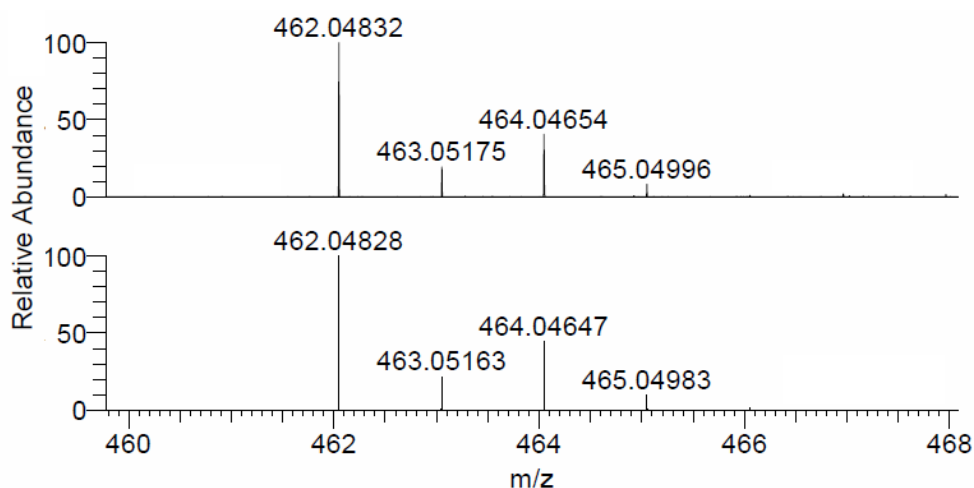
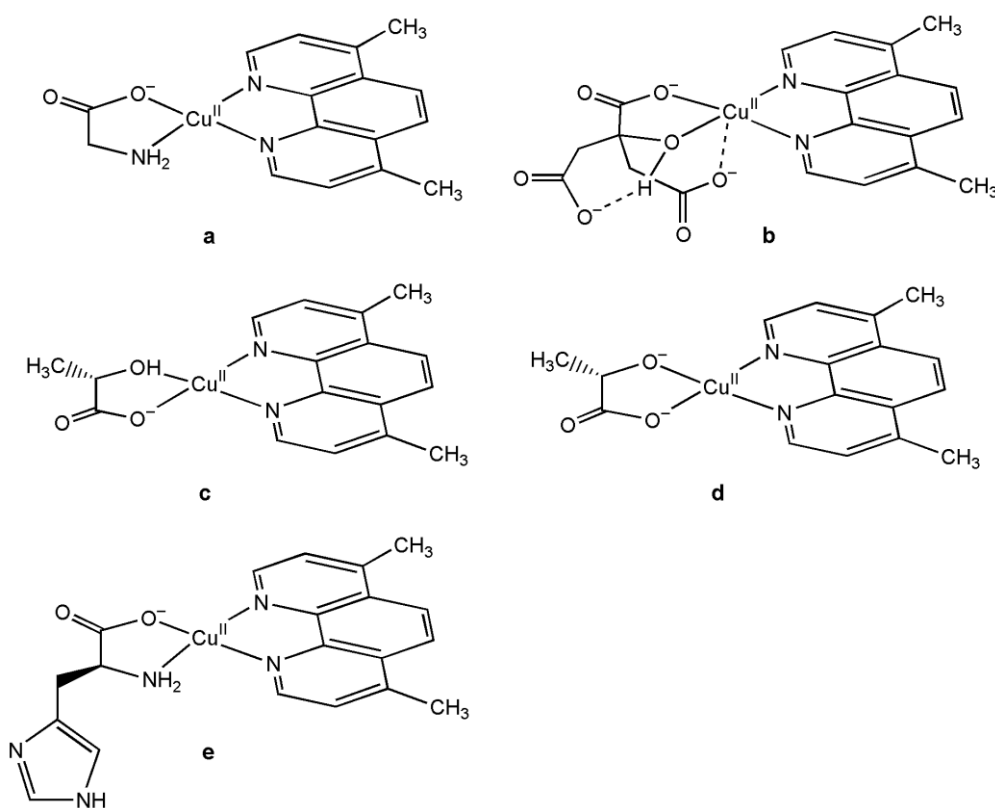


Fig. 5. Experimental (top) and calculated (bottom) isotopic pattern for the $[\text{Cu}^{\text{II}}(\text{Me}_2\text{phen})(\text{citr})+2\text{H}]^+$ peak detected at $m/z = 462.05$ in the ESI-MS(+) spectrum of the $\text{Cu}^{\text{II}}/\text{Me}_2\text{phen}/\text{Gly}/\text{citr}$ 1/1/1/1 system (LC-MS H_2O , Cu^{II} concentration $50 \mu\text{M}$).

EPR spectra, shown in Fig. 6, suggest that at $\text{pH} < 4$ a mixed species is formed in which citrate is in the form citr^{3-} , with the three deprotonated carboxylic groups and the alcohol function protonated (Scheme 2b); the coordination mode is $(\text{N}_{\text{phen}}, \text{N}_{\text{phen}})$; $(\text{COO}^-, \text{OH}, \text{COO}^-_{\text{ax}})$, with citrate binding the metal in a tridentate fashion, and experimental EPR parameters are $g_z = 2.295$ and $A_z(^{63}\text{Cu}) = 169.1 \times 10^{-4} \text{ cm}^{-1}$ (**I** in Fig. 6). Another possibility is the formation of an equatorial seven-membered chelated ring with $(\text{COO}^-, \text{COO}^-)$ coordination. The presence of two coordinated N is confirmed by the superhyperfine coupling revealed in the first parallel resonance, in which a quintuplet with intensity ratio between the lines 1:2:3:2:1 and constant $A(\text{N})$ equal to $10.7 \times 10^{-4} \text{ cm}^{-1}$,

characteristic of the coordination of two nitrogen atoms, is observed. This species is the predominant one in solution up to pH 7.4. $A_2(^{63}\text{Cu})^{\text{calcd}}$ and $A_2(^{14}\text{N})^{\text{calcd}}$ are $172.7 \times 10^{-4} \text{ cm}^{-1}$ and $10.0 \times 10^{-4} \text{ cm}^{-1}$, very close to the experimental values. Notably, ternary species $\text{Cu}^{\text{II}}\text{-phen-citr}$ were observed in the system with phenanthroline [59].

At pH > 9 another complex appears in solution in which citrate is replaced by glycinate to form $[\text{Cu}^{\text{II}}(\text{Me}_2\text{phen})(\text{Gly})]^+$ (**II** in Fig. 6). The finding that the Gly anion with bidentate coordination (NH_2 , COO^-) replaces citrate suggests that the latter is coordinated with the weak $-\text{OH}$ group and not in its stronger deprotonated alcoholato- O^- form. $[\text{Cu}^{\text{II}}(\text{Me}_2\text{phen})(\text{Gly})]^+$ is also revealed by ESI-MS spectrometry.



Scheme 2. Hypothesized structure of the main species revealed in the ternary and quaternary systems studied in this work: (a) $[\text{Cu}^{\text{II}}(\text{Me}_2\text{phen})(\text{Gly})]^+$; (b) $[\text{Cu}^{\text{II}}(\text{Me}_2\text{phen})(\text{citr})]^-$; (c) $[\text{Cu}^{\text{II}}(\text{Me}_2\text{phen})(\text{lact})]^+$; (d) $[\text{Cu}^{\text{II}}(\text{Me}_2\text{phen})(\text{lactH-1})]$; (e) $[\text{Cu}^{\text{II}}(\text{Me}_2\text{phen})(\text{His})]^+$.

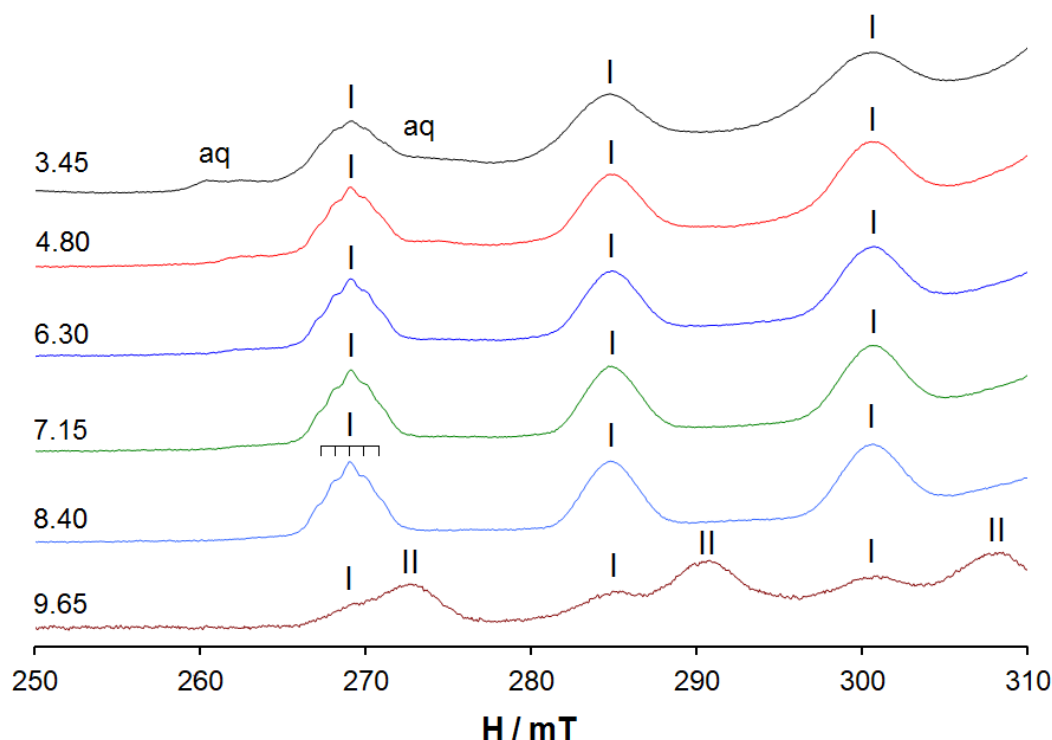


Fig. 6. Low-field region of anisotropic X-band EPR spectra recorded as a function of pH on frozen (120 K) solutions containing $^{63}\text{Cu}^{\text{II}}/\text{Me}_2\text{phen}/\text{Gly}/\text{citr}$ 1/1/1/1 ($^{63}\text{Cu}^{\text{II}}$ concentration 1.0×10^{-3} M). The symbols **aq**, **I** and **II** denote the parallel resonances of aquaion $[\text{Cu}^{\text{II}}(\text{H}_2\text{O})_6]^{2+}$, $[\text{Cu}^{\text{II}}(\text{Me}_2\text{phen})(\text{citr})]^-$ and $[\text{Cu}^{\text{II}}(\text{Me}_2\text{phen})(\text{Gly})]^+$. The position of the quintuplet with ratio 1:2:3:2:1, due to the superhyperfine coupling with ^{14}N , is also shown in the first parallel resonance of the spectrum at pH 8.40.

Table 3. Mixed species identified in the ESI-MS spectra of the systems $\text{Cu}^{\text{II}}/\text{Me}_2\text{phen}/\text{Gly}/bL$ (bL = serum bioligand).

Species	Composition	m/z (exptl) ^a	m/z (calcd) ^a	Deviation (ppm) ^b
$[(\text{Cu}^{\text{II}})_2(\text{Me}_2\text{phen})_2(\text{citr})+\text{H}]^{2+}$	$\text{C}_{34}\text{H}_{30}\text{Cu}_2\text{N}_4\text{O}_7$	366.03496	366.03478	0.5
$[\text{Cu}^{\text{II}}(\text{Me}_2\text{phen})(\text{citr})+2\text{H}]^+$	$\text{C}_{20}\text{H}_{19}\text{CuN}_2\text{O}_7$	462.04832	462.04828	0.1
$[\text{Cu}^{\text{II}}(\text{Me}_2\text{phen})(\text{citr})+\text{H}+\text{Na}]^+$	$\text{C}_{20}\text{H}_{18}\text{CuN}_2\text{NaO}_7$	484.02997	484.03022	-0.5
$[\text{Cu}^{\text{II}}(\text{Me}_2\text{phen})(\text{lact})]^+$	$\text{C}_{17}\text{H}_{17}\text{CuN}_2\text{O}_3$	360.05252	360.05297	-1.2
$[\text{Cu}^{\text{II}}(\text{Me}_2\text{phen})(\text{His})+\text{H}]^{2+}$	$\text{C}_{20}\text{H}_{21}\text{CuN}_5\text{O}_2$	213.04890	213.04901	-0.5
$[\text{Cu}^{\text{II}}(\text{Gly})(\text{His})+\text{H}]^+$	$\text{C}_8\text{H}_{13}\text{CuN}_4\text{O}_4$	292.02260	292.02273	-0.4
$[\text{Cu}^{\text{II}}(\text{Me}_2\text{phen})(\text{His})]^+$	$\text{C}_{20}\text{H}_{20}\text{CuN}_5\text{O}_2$	425.09067	425.09075	-0.2

^a Experimental and calculated m/z values refer to the monoisotopic peak with the highest intensity. ^b Error in ppm with respect to the experimental value, calculated as $10^6 \times [\text{Experimental } (m/z) - \text{Calculated } (m/z)] / \text{Calculated } (m/z)$.

3.2.2. Interaction with L-lactate

In the system with L-lactate, the positive mode ESI-MS spectrum shows the presence of $[\text{Cu}^{\text{II}}(\text{Me}_2\text{phen})(\text{lact})]^+$, for which the m/z value is 360.05 (Table 3 and Fig. S2).

The EPR spectra recorded on the same quaternary system are reported in Fig. 7. As the pH increases, the following species are observed: $[\text{Cu}^{\text{II}}(\text{Me}_2\text{phen})(\text{H}_2\text{O})_4]^+$ (**I**), $[\text{Cu}^{\text{II}}(\text{Me}_2\text{phen})(\text{lact})]^+$ (**II**) and $[\text{Cu}^{\text{II}}(\text{Me}_2\text{phen})(\text{lactH}_{-1})]$ (**III**). The two mixed compounds can be explained, postulating that lactate binds at two equatorial positions with the coordination modes (COO^- , OH) in the adduct **II** and (COO^- , O^-) in **III**. Spin Hamiltonian EPR parameters are $g_z = 2.276$ and $A_z(^{63}\text{Cu}) = 179.1 \times 10^{-4} \text{ cm}^{-1}$ for **II**, and $g_z = 2.245$ and $A_z(^{63}\text{Cu}) = 184.3 \times 10^{-4} \text{ cm}^{-1}$ for **III** (Table 2). The decrease in g_z and increase in $A_z(^{63}\text{Cu})$ for $[\text{Cu}^{\text{II}}(\text{Me}_2\text{phen})(\text{lact})]^+$ compared to $[\text{Cu}^{\text{II}}(\text{Me}_2\text{phen})(\text{citr})]^-$, which has the same equatorial coordination, can be attributed to the absence of the carboxylate group in the axial position (Scheme 2, c). In contrast with citrate, in the spectra with lactate the superhyperfine coupling with nitrogen donors of Me_2phen is not resolved; it is plausible to attribute this finding to the superhyperfine coupling with the hydrogen atoms neighboring to the donors that enlarges the linewidth.

Finally, the deprotonation of the alcohol group in $[\text{Cu}^{\text{II}}(\text{Me}_2\text{phen})(\text{lactH}_{-1})]$ causes the further decrease in g_z and the significant increase in $A_z(^{63}\text{Cu})$ in comparison with $[\text{Cu}^{\text{II}}(\text{Me}_2\text{phen})(\text{lact})]^+$ (Scheme 2, d). The values of $A_z(^{63}\text{Cu})^{\text{calcd}}$ are $175.7 \times 10^{-4} \text{ cm}^{-1}$ for $[\text{Cu}^{\text{II}}(\text{Me}_2\text{phen})(\text{lact})]^+$ and $196.6 \times 10^{-4} \text{ cm}^{-1}$ for $[\text{Cu}^{\text{II}}(\text{Me}_2\text{phen})(\text{lactH}_{-1})]$ with a PD of -1.9% and 6.7%, respectively (Table 2).

It was recently demonstrated that bidentate heterocycle ligands like 1,10-phenanthroline form adducts with Cu^{II} and lactate, even though the structure(s) was(were) not clarified [59].

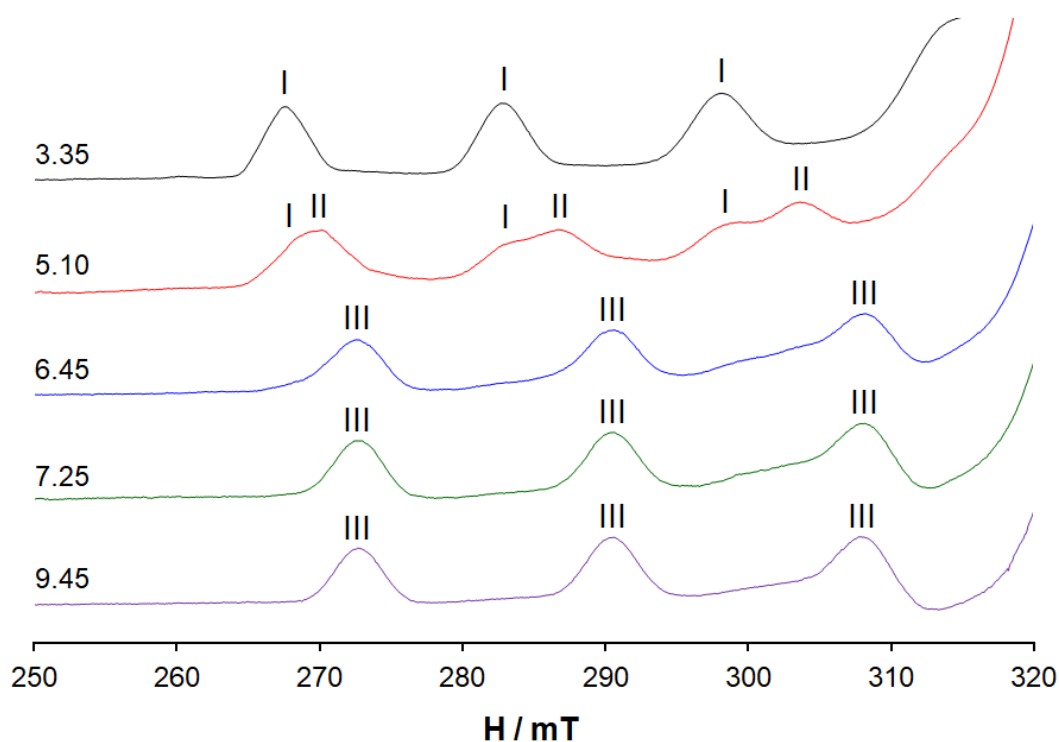


Fig. 7. Low-field region of anisotropic X-band EPR spectra recorded as a function of pH on frozen solutions (120 K) containing $^{63}\text{Cu}^{\text{II}}/\text{Me}_2\text{phen}/\text{Gly}/\text{lact}$ 1/1/1/1 ($^{63}\text{Cu}(\text{II})$ concentration 1.0×10^{-3} M). The symbols **I**, **II**, and **III** denote the parallel resonances of $[\text{Cu}^{\text{II}}(\text{Me}_2\text{phen})(\text{H}_2\text{O})_4]^{2+}$, $[\text{Cu}^{\text{II}}(\text{Me}_2\text{phen})(\text{lact})]^+$ and $[\text{Cu}^{\text{II}}(\text{Me}_2\text{phen})(\text{lactH}_{-1})]$.

3.2.3. Interaction with *L*-histidine

The positive mode ESI-MS spectrum of the $\text{Cu}^{\text{II}}/\text{Me}_2\text{phen}/\text{Gly}/\text{His}$ 1/1/1/1 system is shown in Fig. 8 and the main species identified are listed in Table S3. The formation of $[\text{Cu}^{\text{II}}(\text{Me}_2\text{phen})(\text{Gly})]^+$ and $[\text{Cu}^{\text{II}}(\text{Me}_2\text{phen})(\text{His})]^+$ is observed; for $[\text{Cu}^{\text{II}}(\text{Me}_2\text{phen})(\text{His})]^+$ m/z ratio is 425.09, which was also confirmed by isotopic pattern simulation. This means that, under physiological conditions, amino acids give a mixture of ternary species with $(\text{N}_{\text{phen}}, \text{N}_{\text{phen}}); (\text{NH}_2, \text{COO}^-)$ coordination. Moreover, a species with composition $[\text{Cu}^{\text{II}}(\text{Gly})(\text{His})+\text{H}]^+$ (m/z 292.02) is detected. It is noteworthy that this is the only quaternary system where *bL* (His) is able to partly replace Me_2phen ; solvation energy and hydrogen bonds may explain this finding.

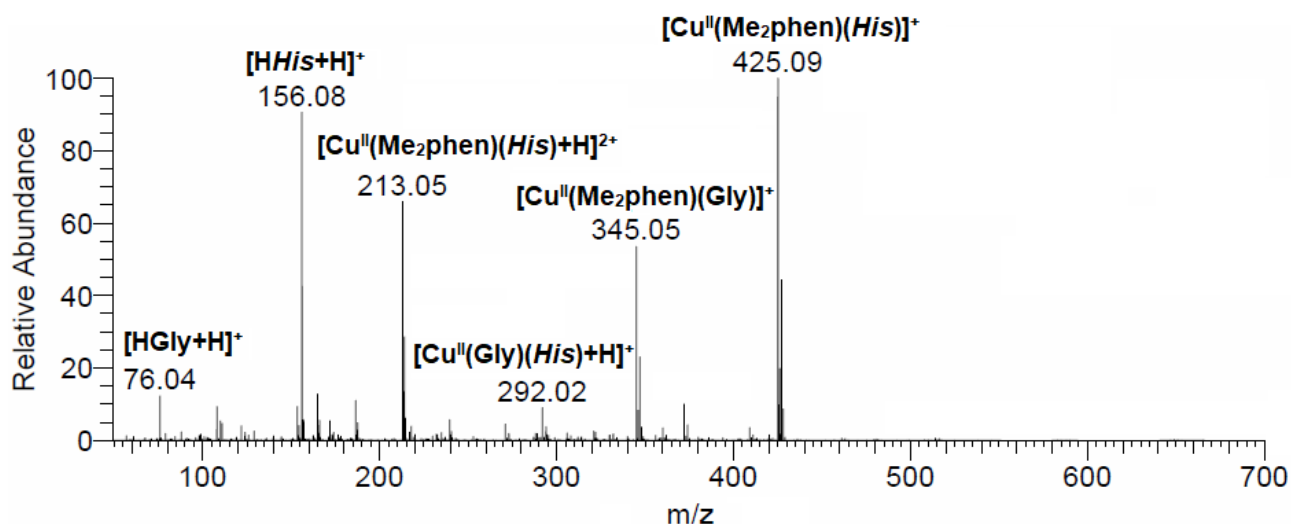


Fig. 8. ESI-MS(+) spectrum recorded on the Cu^{II}/Me₂phen/Gly/His 1/1/1/1 system (LC-MS H₂O, Cu^{II} concentration 50 μM).

EPR spectra indicated the formation of [Cu^{II}(Me₂phen)(H₂O)₄]²⁺ (**I** in Fig. S3) and, at pH greater than 4, the mixed species [Cu^{II}(Me₂phen)(His)]⁺ (**II**). Its spin Hamiltonian parameters are $g_z = 2.244$ and $A_z(^{63}\text{Cu}) = 184.8 \times 10^{-4} \text{ cm}^{-1}$ comparable to those of the analogous complex with glycine, and suggest [(N_{phen}, N_{phen}); (NH₂, COO⁻)] coordination without the axial binding of imidazole nitrogen (Scheme 2e). In the DFT optimized structure, Cu^{II} ion does not interact with imidazole-N (distance 4.118 Å), that forms a hydrogen bond with amino-NH₂ group (1.883 Å), and this could stabilize the structure compared to [Cu^{II}(Me₂phen)(Gly)]⁺. $A_z(^{63}\text{Cu})^{\text{calcd}}$ is $198.0 \times 10^{-4} \text{ cm}^{-1}$ (Table 2). The structure with histamine-like coordination of His (NH₂, N_{imid}) can be excluded because it would have a much larger value of A_z ($208.0 \times 10^{-4} \text{ cm}^{-1}$) and a smaller value of g_z (2.204) compared to the experiment and, moreover, would undergo an unfavorable distortion toward the tetrahedron. Considering the ESI-MS data, the EPR spectra can be interpreted assuming the presence in solution of [Cu^{II}(Me₂phen)(Gly)]⁺ and [Cu^{II}(Me₂phen)(His)]⁺ (**II** in Fig. S3), with L-histidine – behaving as a bidentate ligand – only partially replacing glycinato. In the Cu^{II}/Me₂phen/Gly system, EPR signals of the species with [(N_{phen}, N_{phen}); (NH₂, COO⁻)] coordination are clearly observable only at pH > 7, while the same signals in the quaternary system with His can be detected from pH 5. This can be explained by the presence in solution of two equivalents – instead of only one – of a ligand with donor set (NH₂, COO⁻), stemming both from glycinato and L-histidinato.

At pH 9.55, the resonance around 302 mT are attributed to a dinuclear species, not yet characterized. However, its importance is limited, since it is not observed at pH 7.30 and should disappear at copper concentration lower than that used for EPR experiments (1.0 mM). In fact, this dinuclear complex was not detected by ESI-MS spectra (50 μM), confirming this assumption.

3.3. Binding to cellular bioligands

Inside cellular environment, copper exists as Cu^{I} , while outside exists as Cu^{II} [55]. The conversion mechanism is unclear and consists of a redox reaction, promoted by a thiol compound such as cysteine and *GSH*. It was proposed that the reduction is the key step for the cellular copper uptake *via* high affinity copper transporter protein 1 (Ctr1) and the subsequent binding to cytoplasmatic metallochaperones related to the selective transport to specific organelles [17, 60]. Other reductants could be involved, namely reduced nicotinamide adenine dinucleotide and L-ascorbate.

The redox reactions of copper are closely related to its antitumoral action. In particular, the antiproliferative effect of Cas II-gly is correlated to the intracellular *GSH* that is used as source of electrons to catalyze the Fenton-like reaction [61]. The *GSH* depletion may occur directly by oxidation or indirectly with the production of free radicals upon the reaction with H_2O_2 . A dramatic decrease in intracellular levels of *GSH* was observed in human lung cancer H157 and A549 cells incubated with Cas II-gly [32]. In these cell lines, the metal drug toxicity was enhanced L-buthionine sulfoximine, an inhibitor of *GSH* synthesis, and reduced by Mn(III) with meso-tetrakis(*N,N'*-diethylimidazolium-2-yl)porphyrin, that has an antioxidant catalytic activity [32]. *GSH* depletion is enhanced by L-ascorbic acid and prevented by catalase. Overall, the increase of the ROS concentration upon the Fenton-like reaction causes a depolarization of the mitochondrial membrane, mitochondrial dysfunction and cell death.

3.3.1. Interaction with glutathione

Glutathione is the main cellular reductant and its antioxidant action is related to the ability to be easily oxidized to the corresponding disulfide (*GSSG*). *GSH* and *GSSG* in the neutral form have three and four titratable protons in aqueous solution, respectively.

GSH is potentially capable of binding a metal ion through the amino acid donor set (NH_2 , COO^-) with formation of a five-membered chelate cycle or through monodentate donors such as Cys-S^- or C-terminal residue Gly-COO^- . Formation of other chelate rings is possible only after deprotonation of the amide group(s). In the systems with Cu^{II} , such a deprotonation cannot be ruled out *a priori*, since it is capable of deprotonating the amide bond [62]; nevertheless, the amide deprotonation of the tripeptide could be precluded in the quaternary $\text{Cu}^{\text{II}}/\text{Me}_2\text{phen}/\text{Gly}/\text{GSH}$ system, because 4,7-dimethyl-1,10-phenanthroline and glycinate saturate at least two coordination sites, forcing *GSH* to behave as a bidentate ligand.

The positive-ion mode ESI-MS spectrum shows, in addition to the signal of $[\text{Cu}^{\text{II}}(\text{Me}_2\text{phen})(\text{Gly})]^+$, the presence of $[\text{Cu}^{\text{II}}(\text{Me}_2\text{phen})(\text{GSSG})+4\text{H}]^{2+}$ with $m/z = 441.59$ and

$[(\text{Cu}^{\text{II}})_2(\text{Me}_2\text{phen})_2(\text{GSSG})+2\text{H}]^{2+}$ with $m/z = 576.10$ (see the calculated isotopic pattern in Fig. S4). In addition, the species $[\text{Cu}^{\text{II}}(\text{GSSG})]^{2-}$ with various protonation degrees was detected in both the positive- and negative-ion mode spectra (see Fig. S5 and Table S4).

Table 4. Mixed species identified in the ESI-MS spectra of the systems $\text{Cu}^{\text{II}}/\text{Me}_2\text{phen}/\text{Gly}/cL$ ($cL =$ cellular bioligand).

Species	Composition	m/z (exptl) ^a	m/z (calcd) ^a	Deviation (ppm) ^b
$[\text{Cu}^{\text{II}}(\text{Me}_2\text{phen})(\text{GSSG})+4\text{H}]^{2+}$	$\text{C}_{34}\text{H}_{44}\text{CuN}_8\text{O}_{12}\text{S}_2$	441.59023	441.59026	-0.1
$[(\text{Cu}^{\text{II}})_2(\text{Me}_2\text{phen})_2(\text{GSSG})+2\text{H}]^{2+}$	$\text{C}_{48}\text{H}_{54}\text{Cu}_2\text{N}_{10}\text{O}_{12}\text{S}_2$	576.09726	576.09726	0.0
$[\text{Cu}^{\text{II}}(\text{Me}_2\text{phen})(\text{NADH})+2\text{H}]^{2+}$	$\text{C}_{35}\text{H}_{41}\text{CuN}_9\text{O}_{14}\text{P}_2$	468.07684	468.07666	0.4
$[\text{Cu}^{\text{II}}(\text{Me}_2\text{phen})(\text{NADH})+\text{H}+\text{Na}]^{2+}$	$\text{C}_{35}\text{H}_{40}\text{CuN}_9\text{NaO}_{14}\text{P}_2$	479.06762	479.06763	0.0
$[\text{Cu}^{\text{II}}(\text{Me}_2\text{phen})(\text{NADH})+\text{Cl}]^{-}$	$\text{C}_{35}\text{H}_{39}\text{ClCuN}_9\text{O}_{14}\text{P}_2$	969.11016	969.10817	2.1
$[\text{Cu}^{\text{II}}(\text{Me}_2\text{phen})(\text{NADH})+\text{Cl}+\text{H}_2\text{O}]^{-}$	$\text{C}_{35}\text{H}_{41}\text{ClCuN}_9\text{O}_{15}\text{P}_2$	987.12099	987.11874	2.3
$[\text{Cu}^{\text{II}}(\text{Me}_2\text{phen})(\text{NAD}^+)+\text{H}]^{2+}$ ^c	$\text{C}_{35}\text{H}_{39}\text{CuN}_9\text{O}_{14}\text{P}_2$	467.06906	467.06884	0.5
$[\text{Cu}^{\text{II}}(\text{Me}_2\text{phen})(\text{DHA}_{sc})]^{+}$ ^c	$\text{C}_{20}\text{H}_{17}\text{CuN}_2\text{O}_6$	444.03780	444.03771	0.2
$[\text{Cu}^{\text{II}}(\text{Me}_2\text{phen})(\text{Asc})+\text{H}]^{+}$ ^c	$\text{C}_{20}\text{H}_{19}\text{CuN}_2\text{O}_6$	446.05339	446.05336	0.1
$[\text{Cu}^{\text{II}}(\text{Me}_2\text{phen})(\text{ATP})+3\text{H}+\text{Na}]^{2+}$	$\text{C}_{24}\text{H}_{27}\text{CuN}_7\text{NaO}_{13}\text{P}_3$	400.00289	400.00312	-0.6
$[\text{Cu}^{\text{II}}(\text{Me}_2\text{phen})(\text{ATP})]^{2-}$	$\text{C}_{24}\text{H}_{24}\text{CuN}_7\text{O}_{13}\text{P}_3$	386.99805	386.99760	1.2
$[\text{Cu}^{\text{II}}(\text{Me}_2\text{phen})(\text{ATP})+\text{H}]^{-}$	$\text{C}_{24}\text{H}_{25}\text{CuN}_7\text{O}_{13}\text{P}_3$	775.00415	775.00247	2.2
$[\text{Cu}^{\text{II}}(\text{Me}_2\text{phen})(\text{ADP})]^{-}$ ^d	$\text{C}_{24}\text{H}_{24}\text{CuN}_7\text{O}_{10}\text{P}_2$	695.03750	695.03614	2.0

^a Experimental and calculated m/z values refer to the monoisotopic peak with the highest intensity. ^b Error in ppm with respect to the experimental value, calculated as $10^6 \times [|\text{Experimental } (m/z) - \text{Calculated } (m/z)| / \text{Calculated } (m/z)]$. ^c Very low intensity signal. ^d Species observed in the system $\text{Cu}^{\text{II}}/\text{Me}_2\text{phen}/\text{Gly}/\text{ATP}$.

The formation of the adduct $[(\text{Cu}^{\text{II}})_2(\text{Me}_2\text{phen})_2(\text{GSSG})+2\text{H}]^{2+}$ can be explained with the redox reaction that gives the partial reduction of Cu^{II} to Cu^{I} and oxidation of GSH to GSSG . This was confirmed by the appearance of a dark coloration, which disappeared within a few minutes after the preparation of the solutions. No signals attributable to GSH – but only to its oxidized form GSSG – nor to Cu^{I} were revealed in the mass spectra (see Tables 4 and S4). In contrast, complexes $\text{Cu}^{\text{II}}-\text{GSH}$ were isolated in the solid state [63].

EPR spectra recorded on frozen solutions containing $^{63}\text{Cu}^{\text{II}}/\text{Me}_2\text{phen}/\text{Gly}/\text{GSH}$ at a molar ratio of 1/1/1/1 show, with varying pH, the presence of two major species that can be identified with the mono-chelated complex formed by Me_2phen with coordination mode $(\text{N}_{\text{phen}}, \text{N}_{\text{phen}}); 4\text{H}_2\text{O}$, denoted with **I** in Fig. 9, and another with $(\text{N}_{\text{phen}}, \text{N}_{\text{phen}}); (\text{NH}_2, \text{COO}^-)$, **II**, with $g_z = 2.241$ and $A_z(^{63}\text{Cu}) = 187.0 \times 10^{-4} \text{ cm}^{-1}$, very similar to $[\text{Cu}^{\text{II}}(\text{Me}_2\text{phen})(\text{Gly})]^{+}$ (see Table 2). This means that a mixture

of $[\text{Cu}^{\text{II}}(\text{Me}_2\text{phen})(\text{Gly})]^+$ and $[\text{Cu}^{\text{II}}(\text{Me}_2\text{phen})(\text{H}_x\text{GSSG})]^{(x-2)+}$, with $x = 0-3$, may exist in solution with Gly or GSSG binding copper(II) through the amino acid donor set.

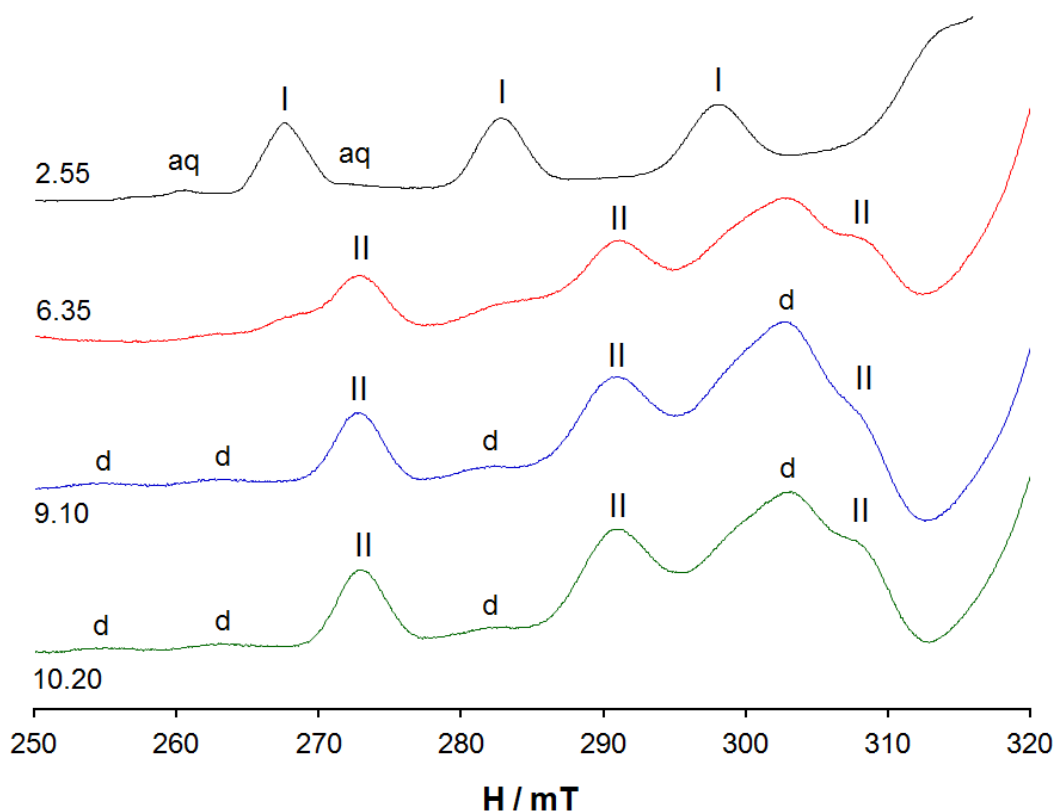
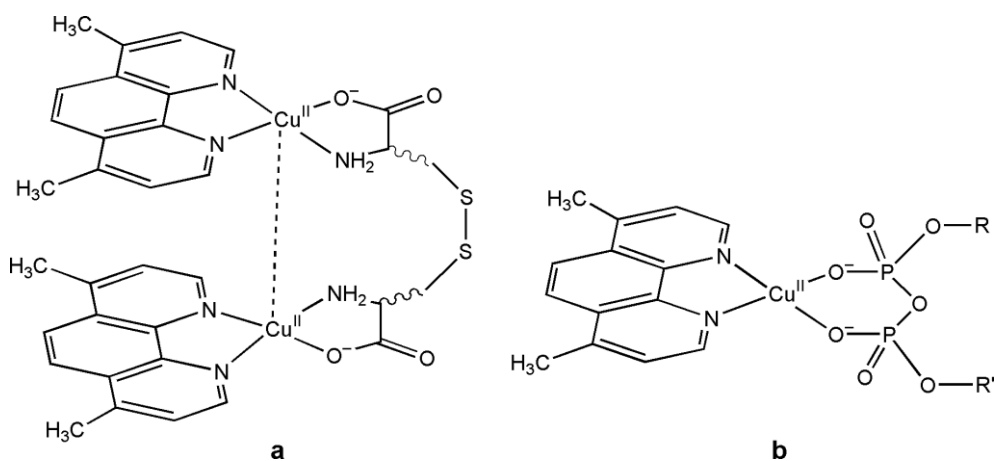


Fig. 9. Low-field region of anisotropic X-band EPR spectra recorded as a function of pH on frozen solutions (120 K) containing $^{63}\text{Cu}^{\text{II}}/\text{Me}_2\text{phen}/\text{Gly}/\text{GSH}$ 1/1/1/1 (Cu^{II} concentration 1.0×10^{-3} M). The symbols **aq**, **I** and **II** are indicated the parallel resonances of $[\text{Cu}^{\text{II}}(\text{H}_2\text{O})_6]^{2+}$, $[\text{Cu}^{\text{II}}(\text{Me}_2\text{phen})(\text{H}_2\text{O})_4]^{2+}$ and $[\text{Cu}^{\text{II}}(\text{Me}_2\text{phen})(\text{Gly})]^+ / [\text{Cu}^{\text{II}}(\text{Me}_2\text{phen})(\text{H}_x\text{GSSG})]^{(x-2)+}$, with $x = 0-3$. With the letter **d** the resonances of the dinuclear species $[(\text{Cu}^{\text{II}})_2(\text{Me}_2\text{phen})_2(\text{H}_x\text{GSSG})]^{x+}$, with $x = 0-2$, are indicated.

In addition to these species, it is also possible to identify the EPR resonances (indicated by the letter **d** in Fig. 9) that cannot be attributed to a mononuclear Cu^{II} complex, but to a dinuclear structure, as confirmed by the signals with g around to 4 observed at half-field between 120 and 180 mT (Fig. S6), clearly indicative of a magnetic interaction between two paramagnetic Cu^{II} centers and ascribable to $\Delta M_s = \pm 2$ transitions [64]. The information that can be extracted from the signals detected at g ca. 2 does not allow to characterize the species responsible for these absorptions, but it can be stated that the formation of the dinuclear complex is certainly related to the presence of glutathione in solution, because it is not observed in the corresponding $\text{Cu}^{\text{II}}/\text{Me}_2\text{phen}/\text{Gly}$ ternary system. Considering that ESI-MS spectrometry did not reveal species with the reduced form of

glutathione, it is plausible that only *GSSG* and not *GSH* binds to copper, coordinating more than one ion at the same time. The detection of $[(\text{Cu}^{\text{II}})_2(\text{Me}_2\text{phen})_2(\text{GSSG})+2\text{H}]^{2+}$ by MS studies suggests that the structure of the dimeric species could have two $\text{Cu}^{\text{II}}(\text{Me}_2\text{phen})^{2+}$ moieties bound by (NH_2 , COO^-) donor set of the γ -glutamate residue to form a dinuclear adducts with the two Cu^{II} ions interacting ferromagnetically (Scheme 3, a). The stoichiometry would be $[(\text{Cu}^{\text{II}})_2(\text{Me}_2\text{phen})_2(\text{H}_x\text{GSSG})]^{x+}$, with $x = 0-2$, depending on the protonation degree of *GSSG*.



Scheme 3. Structure of: a) the dinuclear species $[(\text{Cu}^{\text{II}})_2(\text{Me}_2\text{phen})_2(\text{H}_x\text{GSSG})]^{x+}$, with $x = 0-3$, and b) $[\text{Cu}^{\text{II}}(\text{Me}_2\text{phen})_2(\text{H}_x\text{NADH})]^{x+}$ ($x = 0-2$) / $[\text{Cu}^{\text{II}}(\text{Me}_2\text{phen})_2(\text{H}_x\text{NAD}^+)]^{(x+1)+}$ ($x = 0-1$) / $[\text{Cu}^{\text{II}}(\text{Me}_2\text{phen})_2(\text{H}_x\text{ATP})]^{(x-2)}$ ($x = 0-4$). With *NADH* and *NAD*⁺ R is adenosine and R' is nicotinamide riboside, while with *ATP* R is adenosine phosphate and R' is simply a negative charge.

To characterize the dinuclear complex, the structure of $[(\text{Cu}^{\text{II}})_2(\text{Me}_2\text{phen})_2(\text{GSSG})]$ was DFT optimized and the magnetic coupling between the two Cu^{II} ions calculated. The structure (Fig. S7) shows that the distance between two coppers is 4.06 Å and that the interaction is favored by the π - π stacking between the aromatic system of the two Me_2phen molecules; the distance between the centroids of the two planes is 3.42 Å. The magnetic interaction is weakly ferromagnetic, in agreement with EPR data, with a predicted value of J of 1.6 cm^{-1} .

3.3.2. Interaction with *NADH*

NADH and its oxidized form *NAD*⁺ are crucial coenzymes for the metabolic processes and are involved in many redox reactions. They possess the central diphosphate group able to bind metal ions. In this study, the system $\text{Cu}^{\text{II}}/\text{Me}_2\text{phen}/\text{Gly}/\text{NADH}$ 1/1/1/1 was investigated. The adducts of $[\text{Cu}^{\text{II}}(\text{Me}_2\text{phen})(\text{NADH})]$ with H^+ , Na^+ and Cl^- were detected in the ESI-MS spectra. The comparison of the experimental and calculated isotopic pattern of $[\text{Cu}^{\text{II}}(\text{Me}_2\text{phen})(\text{NADH})+2\text{H}]^{2+}$, is

shown in Fig. S8. Notably, as in the system with *GSH*, a redox process is observed with formation of NAD^+ , that in part coordinates copper forming $[Cu^{II}(Me_2phen)(NAD^+)+H]^{2+}$; moreover, $[NAD^++2H]^+$ and $[(NAD^+)+H+Na]^+$ are detected (Table 4 and S5). The possible structure of the adducts with *NADH* and NAD^+ is reported in Scheme 3, b.

EPR spectra are reported in Fig. S9. $[Cu^{II}(Me_2phen)(H_2O)_4]^{2+}$ (**I**) is detected at pH around 3 and, with increasing pH, a small amount of $[Cu^{II}(Me_2phen)(H_xNADH)]^{x+}$, with $x = 0-2$ (**II**) or, alternatively, $[Cu^{II}(Me_2phen)(H_xNAD^+)]^{(x+1)+}$, with $x = 0-1$, is formed. The values of g_z and $A_z(^{63}Cu)$ are 2.300 and $168.9 \times 10^{-4} \text{ cm}^{-1}$, respectively. Since the two species would have the same coordination mode, it is not possible to distinguish them by EPR spectroscopy. However, on the basis of the EPR data, $Cu^{II}-Me_2phen-(NADH/NAD^+)$ adducts should exist in a lower amount than $[Cu^{II}(Me_2phen)(H_xGSSG)]^{(x-2)+}$ due to the low basicity of the diphosphate group compared to the (NH_2, COO^-) couple. At pH higher than 7, $[Cu^{II}(Me_2phen)(Gly)]^+$ (**III**) is observed.

Interesting observations can be made comparing the behavior of the systems with *GSH* and *NADH*: i) in the ESI-MS spectra with *GSH* only free *GSSG* is observed, while with *NADH* both this latter and NAD^+ are detected and ii) the only adducts in the system with *GSH* are formed with *GSSG*, while with *NADH* the adducts are formed with *NADH* and NAD^+ , suggesting that the redox reaction occurs more with *GSH* than with *NADH*. Moreover, in both the systems, Cu^I does not give complexation probably because it is a 'soft' ion compared to Cu^{II} and has little affinity for nitrogen and oxygen donors.

3.3.3. Interaction with ascorbate

In the system with L-ascorbic acid, ternary species are not observed in appreciable concentration. However, as with *GSH* and *NADH*, a redox process takes place with formation of the oxidized derivative, dehydroascorbic acid (*DHAsc*). Notably, in the ESI-MS spectra, $[HAsc]^-$ and $[DHAsc]^-$ are detected at m/z 175.02 and 173.01, while the hydrolysis product of this latter, 2,3-diketo-L-gulonate $[HDKG+Cl]^-$ at m/z 227.00. Instead, the peaks of $[Cu^{II}(Me_2phen)(DHAsc)]^+$ and $[Cu^{II}(Me_2phen)(Asc)+H]^+$ are revealed in a very small amounts (Tables 4 and S6, and Fig. S10). This could be related to the weak complexing behavior of L-ascorbate and dehydroascorbate that, around at physiological pH, do not show high affinity toward the transition metal ions. No signals attributable to Cu^I were detected.

3.3.4. Interaction with ATP

ATP is able to bind a metal ions in acidic media through the triphosphate moiety and in alkaline solution through the vicinal *cis*-hydroxyl groups of the ribose group [65].

ESI-MS(+) spectrum of the quaternary system containing Cas II-gly and *ATP* showed a cationic complex with *m/z* ratio of 400.00, coincident with $[\text{Cu}^{\text{II}}(\text{Me}_2\text{phen})(\text{ATP})+3\text{H}+\text{Na}]^{2+}$. ESI-MS(-) experiments (Fig. 10) allowed us to detect two adducts with Cu^{II} , Me_2phen and *ATP*: $[\text{Cu}^{\text{II}}(\text{Me}_2\text{phen})(\text{ATP})+\text{H}]^-$ and $[\text{Cu}^{\text{II}}(\text{Me}_2\text{phen})(\text{ATP})]^{2-}$. The experimental and calculated isotopic pattern is represented Fig. S11, while all the species are listed in Table S7. Notably, in the ionization process *ADP* is formed and this binds the $\text{Cu}^{\text{II}}(\text{Me}_2\text{phen})^{2+}$ moiety. At the moment, it is not known if the formation of *ADP* is due to the partial hydrolysis of *ATP* promoted by Cu^{II} or occurs in-source during the recording of the spectrum.

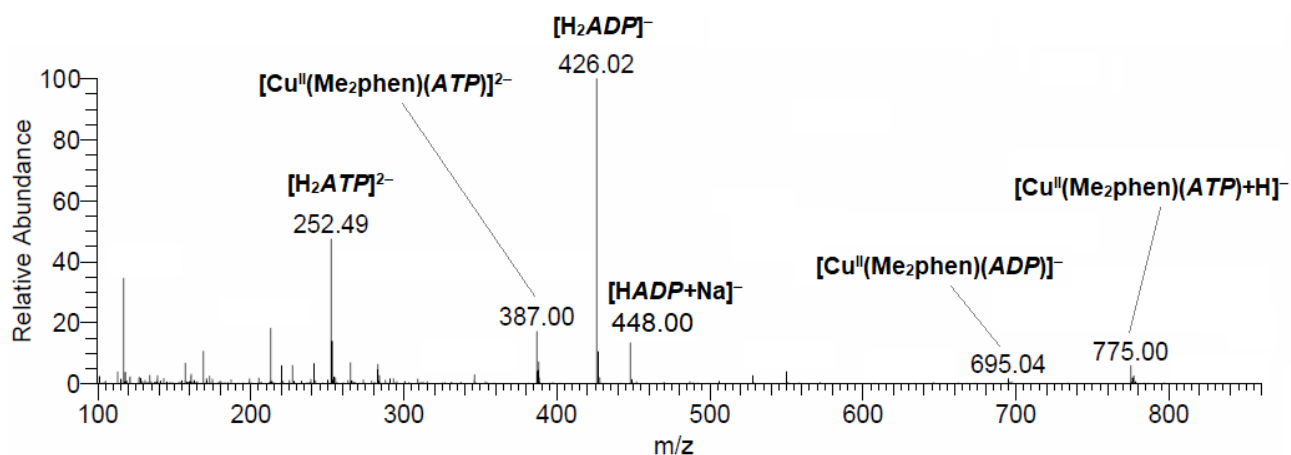


Fig. 10. ESI-MS(-) spectrum recorded on the $\text{Cu}^{\text{II}}/\text{Me}_2\text{phen}/\text{Gly}/\text{ATP}$ 1/1/1/1 (LC-MS H_2O , Cu^{II} concentration 50 μM).

The EPR spectra show the stepwise formation of $[\text{Cu}^{\text{II}}(\text{Me}_2\text{phen})(\text{H}_2\text{O})_4]^{2+}$ (**I** in Fig. 11) at very acid values, $[\text{Cu}^{\text{II}}(\text{Me}_2\text{phen})_2(\text{H}_x\text{ATP})]^{(x-2)}$, with $x = 0-4$ (**II**), in which the deprotonation of phosphoric group depends on the pH, and $[\text{Cu}^{\text{II}}(\text{Me}_2\text{phen})(\text{Gly})]^+$ (**III**) above pH 10. It is interesting to observe that the mixed complex with *ATP* predominates from pH 5 to 10 and is the only species in solution at physiological pH. Its experimental EPR parameters are $g_z = 2.291$ and $A_z(^{63}\text{Cu}) = 169.9 \times 10^{-4} \text{ cm}^{-1}$, while the calculated ones are $g_z^{\text{calcd}} = 2.228$ and $A_z(^{63}\text{Cu})^{\text{calcd}} = 181.3 \times 10^{-4} \text{ cm}^{-1}$.

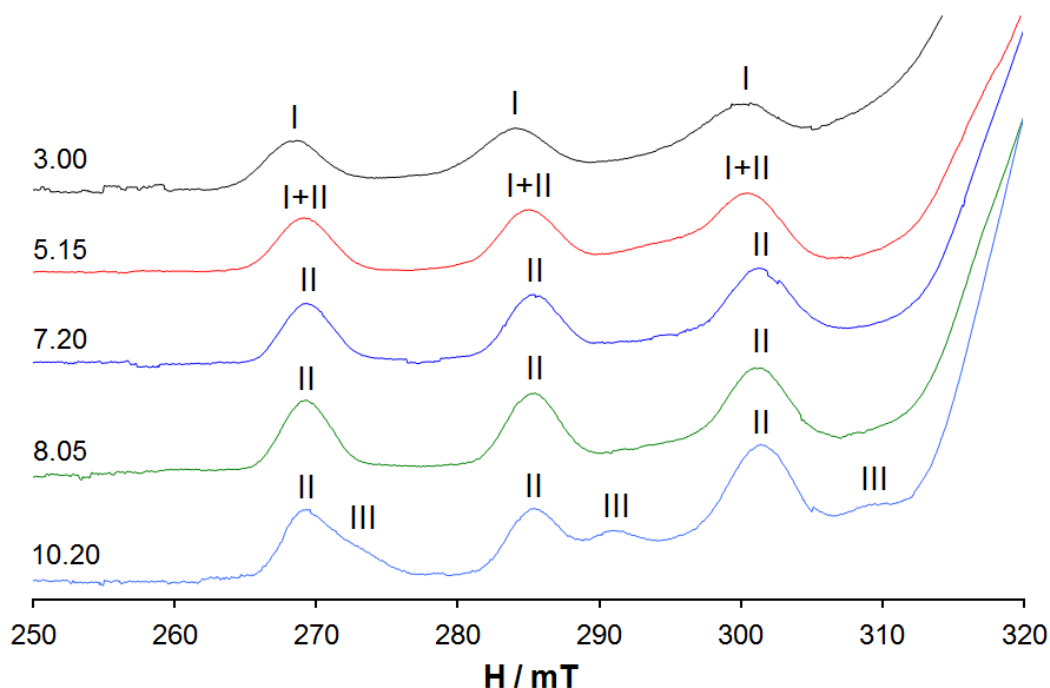


Fig. 11. Low-field region of anisotropic X-band EPR spectra recorded as a function of pH on frozen solutions (120 K) containing $^{63}\text{Cu}^{\text{II}}/\text{Me}_2\text{phenGly}/\text{ATP}$ 1/1/1/1 (Cu^{II} concentration 1.0×10^{-3} M). The symbols **I**, **II** and **III** indicate the parallel resonances of $[\text{Cu}^{\text{II}}(\text{Me}_2\text{phen})(\text{H}_2\text{O})_4]^{2+}$, $[\text{Cu}^{\text{II}}(\text{Me}_2\text{phen})_2(\text{H}_x\text{ATP})]^{(x-2)}$, with $x = 0-4$, and $[\text{Cu}^{\text{II}}(\text{Me}_2\text{phen})(\text{Gly})]^+$.

4. Conclusions

Casiopeinas® constitute a family of patented mixed Cu^{II} complexes with antitumor pharmacological activity, having general formula $[\text{Cu}^{\text{II}}(\text{L}^{\text{N-N}})(\text{L}'^{\text{N-O}})]\text{NO}_3$. Among the most active Casiopeinas®, Cas II-gly with $\text{L}^{\text{N-N}} = \text{Me}_2\text{phen}$ and $\text{L}'^{\text{N-O}} = \text{glycinato}$ is worth of being mentioned and has been studied in this work.

The mode of action of Casiopeinas® and active species in the organism has not been fully elucidated and remains unclear. The transport in blood of these compounds and the form in which they reach the target cells is a relevant issue because biological action may depend on this. In the biological fluids, Cas II-gly can keep its identity or undergo several reactions: the replacement of Me_2phen or Gly by serum or cytosol bioligands (bL or cL) or both of them to form possible mixed species $\text{Cu}^{\text{II}}\text{-Me}_2\text{phen-bL/cL}$, $\text{Cu}^{\text{II}}\text{-Gly-bL/cL}$, or $\text{Cu}^{\text{II}}\text{-bL/cL}$. These reactions may preclude the achievement of cellular targets or, conversely, may facilitate the crossing of cell membranes. Therefore, it is essential to know the transformation of Casiopeinas® in the blood serum or in the cellular environment to identify the possible active complex(es) in the organism.

In this study we demonstrated that most of blood and cytosol bioligands could replace partly or completely glycinate to form $\text{Cu}^{\text{II}}\text{-Me}_2\text{phen-}bL/cL$. With amino acid, a mixture of mixed species with $(\text{N}_{\text{phen}}, \text{N}_{\text{phen}})$; $(\text{NH}_2, \text{COO}^-)$ coordination is formed. In the system with *GSH*, *NADH* and ascorbate, a redox reaction with the partial oxidation of *cL* to *GSSG*, NAD^+ and dehydroascorbate and formation of Cu^{I} is observed. The oxidized form of the bioligands can interact with Cu^{II} , the results indicating that *GSSG* is the stronger ligand followed by NAD^+ and dehydroascorbate. The reduced Cu^{I} ion does not yield ternary adducts, probably for its ‘soft’ character compared to Cu^{II} and its scarce affinity for nitrogen and oxygen donors, but could promote Fenton-like reactions with production of reactive oxygen species related to the antitumor activity of Casiopeinas®. These findings are in line with the data in literature for which copper occurs as Cu^{I} inside the cells, and as Cu^{II} outside. The mechanism of conversion consists of a not completely clear redox reaction, in which a thiol compound such as *GSH* or cysteine could be involved. On the basis of our results, it is plausible that also *NADH* and L-ascorbate contribute to the process. As pointed out in the literature [17], the reduction to Cu^{I} may be the driving force that promotes the cellular copper uptake and its speciation and eventual transformation in the cytosol.

It is not clear the fate of $\text{Cu}^{\text{II}}\text{-Me}_2\text{phen}$ moiety inside the cells. Costa Pessoa and co-workers have recently demonstrated that in the $\text{Cu}^{\text{II}}/\text{phen}$ systems the interaction with cell components and subsequent cell death involves the separate action of copper(II) ions and phen ligand and not of the $\text{Cu}^{\text{II}}\text{-phen}$ species. It is reasonable to think, even considering the results obtained in the $\text{V}^{\text{IV}}\text{O}/\text{phen}$ systems [66, 67], that a mixture of species can contribute to the transport and biological activity of Casiopeinas®.

Considering that only equimolar solutions containing Cas II-gly and the bioligands were used in the present paper, in the next future these systems will be investigated using the relative physiological concentration of *bL* and *cL* and the copper biospeciation in real serum samples. Moreover, the behavior of the Casiopeinas® will be studied in the presence of the proteins to evaluate if these latter may affect the biospeciation of copper.

Conflicts of interest

There are no conflicts to declare.

Supplementary Material

Supplementary data to this article can be found online at <http://dx.doi.org/10.1016/j.jinorgbio.2021.xx.xxx>.

Acknowledgements

The authors thank Regione Autonoma della Sardegna (grant RASSR79857) and Fondazione di Sardegna (grant 2017) for the financial support.

5. References

- [1] K.D. Karlin, Z. Tyeklár, *Bioinorganic Chemistry of Copper*, Chapman & Hall, Inc., New York, NY, 1993.
- [2] R.A. Festa, D.J. Thiele, *Curr. Biol.* 21 (2011) R877-R883.
- [3] W. Maret, A. Wedd, *Binding, Transport and Storage of Metal Ions in Biological Cells*, The Royal Society of Chemistry, 2014.
- [4] D. Rehder, *Bioinorganic Chemistry*, Oxford University Press, Oxford, 2014.
- [5] G. Crisponi, V.M. Nurchi, D. Fanni, C. Gerosa, S. Nemolato, G. Faa, *Coord. Chem. Rev.* 254 (2010) 876-889.
- [6] C. Marzano, M. Pellei, F. Tisato, C. Santini, *Anti-Cancer Agents Med. Chem.* 9 (2009) 185-211.
- [7] A. Hussain, M.F. AlAjmi, M.T. Rehman, S. Amir, F.M. Husain, A. Alsalmeh, M.A. Siddiqui, A.A. AlKhedhairi, R.A. Khan, *Sci. Rep.* 9 (2019) 5237.
- [8] F. Tisato, C. Marzano, M. Porchia, M. Pellei, C. Santini, *Med. Res. Rev.* 30 (2010) 708-749.
- [9] I. Iakovidis, I. Delimaris, S.M. Piperakis, *Mol. Biol. Int.* (2011) 594529.
- [10] C. Santini, M. Pellei, V. Gandin, M. Porchia, F. Tisato, C. Marzano, *Chem. Rev.* 114 (2014) 815-862.
- [11] A. Kellett, Z. Molphy, V. McKee, C. Slator, *Recent Advances in Anticancer Copper Compounds*, in: A. Casini, A. Vessières, S.M. Meier-Menches (Eds.), *Metal-based Anticancer Agents*, The Royal Society of Chemistry, Croydon, United Kingdom, 2019, pp. 91-119.
- [12] A. Bergamo, G. Sava, *Chem. Soc. Rev.* 44 (2015) 8818-8835.
- [13] X. Huiqi, Y.J. Kang, *Curr. Med. Chem.* 16 (2009) 1304-1314.
- [14] A.R. Mufti, E. Burstein, C.S. Duckett, *Arch. Biochem. Biophys.* 463 (2007) 168-174.
- [15] C.R. Kowol, P. Heffeter, W. Miklos, L. Gille, R. Trondl, L. Cappellacci, W. Berger, B.K. Keppler, *JBIC, J. Biol. Inorg. Chem.* 17 (2012) 409-423.
- [16] S. Medici, M. Peana, V.M. Nurchi, J.I. Lachowicz, G. Crisponi, M.A. Zoroddu, *Coord. Chem. Rev.* 284 (2015) 329-350.
- [17] T. Kiss, É.A. Enyedy, T. Jakusch, *Coord. Chem. Rev.* 352 (2017) 401-423.
- [18] C. Rivera-Guevara, M.E. Bravo-Gómez, L. Ruiz-Azuara, *Chemotherapy and Design of New Antineoplastic Compounds*, in: J. Camacho (Ed.), *Molecular Oncology: Principles and Recent Advances*, Bentham, 2012, pp. 172-191.
- [19] X. Solans, L. Ruiz-Ramirez, A. Martinez, L. Gasque, J.L. Brioso, *Acta Crystallogr., Sect. C: Cryst. Struct. Commun.* 44 (1988) 628-631.

- [20] X. Solans, L. Ruiz-Ramirez, A. Martinez, L. Gasque, R. Moreno-Esparza, *Acta Crystallogr., Sect. C: Cryst. Struct. Commun.* 48 (1992) 1785-1788.
- [21] X. Solans, L. Ruiz-Ramirez, A. Martinez, L. Gasque, R. Moreno-Esparza, *Acta Crystallogr., Sect. C: Cryst. Struct. Commun.* 49 (1993) 890-893.
- [22] L. Ruiz-Azuara, 07/628,628: Re 635,458. 1992, USA.
- [23] L. Ruiz-Azuara, 07/628,843: RE 635,458, Feb. 618 (1997). 1992, United States Patent.
- [24] L. Ruiz-Azuara, 07/628,628: 625,576,326.1996, United States Patent.
- [25] M. Chikira, Y. Tomizawa, D. Fukita, T. Sugizaki, N. Sugawara, T. Yamazaki, A. Sasano, H. Shindo, M. Palaniandavar, W.E. Antholine, *J. Inorg. Biochem.* 89 (2002) 163-173.
- [26] M. Chikira, C.H. Ng, M. Palaniandavar, *Int. J. Mol. Sci.* 16 (2015) 22754-22780.
- [27] W.L. Kwik, K.P. Ang, G. Chen, *J. Inorg. Nucl. Chem.* 42 (1980) 303-313.
- [28] L. Gasque, R. Moreno-Esparza, L. Ruiz-Ramírez, *J. Inorg. Biochem.* 48 (1992) 121-127.
- [29] M.E. Bravo-Gómez, J.C. García-Ramos, I. Gracia-Mora, L. Ruiz-Azuara, *J. Inorg. Biochem.* 103 (2009) 299-309.
- [30] T.J. Wadas, E.H. Wong, G.R. Weisman, C.J. Anderson, *Curr. Pharm. Des.* 13 (2007) 3-16.
- [31] C. Mejia, L. Ruiz-Azuara, *Pathol. Oncol. Res.* 14 (2008) 467-472.
- [32] R. Kachadourian, H.M. Brechbuhl, L. Ruiz-Azuara, I. Gracia-Mora, B.J. Day, *Toxicology* 268 (2010) 176-183.
- [33] I. Correia, S. Borovic, I. Cavaco, C.P. Matos, S. Roy, H.M. Santos, L. Fernandes, J.L. Capelo, L. Ruiz-Azuara, J. Costa Pessoa, *J. Inorg. Biochem.* 175 (2017) 284-297.
- [34] W.R. Harris, *Clin. Chem.* 38 (1992) 1809-1818.
- [35] Williams Hematology, 8th Ed, The McGraw-Hill Co., Inc., China, 2010.
- [36] In the text the bioligands are indicated in italic font with their general abbreviation and the fully deprotonated form in aqueous solution is used: *citr(3-)*, *lact(-)*, *His(-)*, *GSH(3-)*, *GSSG(4-)*, *NADH(2-)*, *NAD⁺(-)*, *Asc(2-)*, *DHAsc(-)*, *DKG(-)*, *ATP(4-)*, *ADP(3-)*.
- [37] M.J. Frisch, G.W. Trucks, H.B. Schlegel, G.E. Scuseria, M.A. Robb, J.R. Cheeseman, G. Scalmani, V. Barone, B. Mennucci, G.A. Petersson, H. Nakatsuji, M. Caricato, X. Li, H.P. Hratchian, A.F. Izmaylov, J. Bloino, G. Zheng, J.L. Sonnenberg, M. Hada, M. Ehara, K. Toyota, R. Fukuda, J. Hasegawa, M. Ishida, T. Nakajima, Y. Honda, O. Kitao, H. Nakai, T. Vreven, J.A. Montgomery, Jr., J.E. Peralta, F. Ogliaro, M. Bearpark, J.J. Heyd, E. Brothers, K.N. Kudin, V.N. Staroverov, T. Keith, R. Kobayashi, J. Normand, K. Raghavachari, A. Rendell, J.C. Burant, S.S. Iyengar, J. Tomasi, M. Cossi, N. Rega, J.M. Millam, M. Klene, J.E. Knox, J.B. Cross, V. Bakken, C. Adamo, J. Jaramillo, R. Gomperts, R.E. Stratmann, O. Yazyev, A.J. Austin, R. Cammi, C. Pomelli, J.W. Ochterski, R.L. Martin, K. Morokuma, V.G. Zakrzewski, G.A. Voth, P. Salvador, J.J.

- Dannenberg, S. Dapprich, A.D. Daniels, Ö. Farkas, J.B. Foresman, J.V. Ortiz, J. Cioslowski, D.J. Fox, Gaussian 09, revision D.01, Gaussian, Inc., Wallingford, CT, 2010.
- [38] A.D. Becke, *J. Chem. Phys.* 98 (1993) 5648-5652.
- [39] C. Lee, W. Yang, R.G. Parr, *Phys. Rev. B* 37 (1988) 785-789.
- [40] M. Bühl, H. Kabrede, *J. Chem. Theory Comput.* 2 (2006) 1282-1290.
- [41] M. Bühl, C. Reimann, D.A. Pantazis, T. Bredow, F. Neese, *J. Chem. Theory Comput.* 4 (2008) 1449-1459.
- [42] A.V. Marenich, C.J. Cramer, D.G. Truhlar, *J. Phys. Chem. B* 113 (2009) 6378-6396.
- [43] F. Neese, *Wiley Interdiscip. Rev. Comput. Mol. Sci.* 8 (2017) e1327.
- [44] J.P. Perdew, K. Burke, M. Ernzerhof, *Phys. Rev. Lett.* 77 (1996) 3865-3868.
- [45] J.P. Perdew, K. Burke, M. Ernzerhof, *Phys. Rev. Lett.* 78 (1997) 1396-1396.
- [46] G. Sciortino, G. Lubinu, J.-D. Maréchal, E. Garribba, *Magnetochemistry* 4 (2018) 55.
- [47] A. Rodríguez-Forteza, P. Alemany, S. Alvarez, E. Ruiz, *Eur. J. Inorg. Chem.* 2004 (2004) 143-153.
- [48] E. Ruiz, J. Cano, S. Alvarez, P. Alemany, *J. Comput. Chem.* 20 (1999) 1391-1400.
- [49] C. Hao, R.E. March, *J. Mass Spectrom.* 36 (2001) 509-521.
- [50] D. Sanna, P. Buglyo, A.I. Tomaz, J.C. Pessoa, S. Borovic, G. Micera, E. Garribba, *Dalton Trans.* 41 (2012) 12824-12838.
- [51] J. Peisach, W.E. Blumberg, *Arch. Biochem. Biophys.* 165 (1974) 691-708.
- [52] F. Neese, *J. Chem. Phys.* 118 (2003) 3939-3948.
- [53] D. İnci, R. Aydın, Ö. Vatan, T. Sevgi, D. Yılmaz, Y. Zorlu, Y. Yerli, B. Çoşut, E. Demirkan, N. Çinkılıç, *JBIC, J. Biol. Inorg. Chem.* 22 (2017) 61-85.
- [54] A. Levina, D.C. Crans, P.A. Lay, *Coord. Chem. Rev.* 352 (2017) 473-498.
- [55] T. Kiss, É.A. Enyedy, T. Jakusch, O. Dömötör, *Curr. Med. Chem.* 26 (2019) 580-606.
- [56] T. Jakusch, T. Kiss, *Coord. Chem. Rev.* 351 (2017) 118-126.
- [57] D. Sanna, V. Ugone, G. Micera, P. Buglyó, L. Bíró, E. Garribba, *Dalton Trans.* 46 (2017) 8950-8967.
- [58] E.R. Still, P. Wikberg, *Inorg. Chim. Acta* 46 (1980) 147-152.
- [59] A. Nobrega, V.R. Landaeta, R. Rodriguez-Lugo, M.L. Araujo, W. Madden, L. Hernández, V. Lubes, *Phys. Chem. Liq.* (2021) 1-13.
- [60] J.B. Blackburn, N. Yan, S. Lutsenko, *Copper in Eukaryotes*, in: W. Maret, A. Wedd (Eds.), *Binding, Transport and Storage of Metal Ions in Biological Cells*, The Royal Society of Chemistry, Cambridge, 2014, pp. 524-555.

- [61] R. Alemón-Medina, M.E. Bravo-Gómez, M.I. Gracia-Mora, L. Ruiz-Azuara, *Toxicol. in Vitro* 25 (2011) 868-873.
- [62] H. Sigel, R.B. Martin, *Chem. Rev.* 82 (1982) 385-426.
- [63] D.N. Kumar, B.K. Singh, B.S. Garg, P.K. Singh, *Spectrochim. Acta A Mol. Biomol. Spectrosc.* 59 (2003) 1487-1496.
- [64] T.D. Smith, J.R. Pilbrow, *Coord. Chem. Rev.* 13 (1974) 173-278.
- [65] E. Alberico, D. Dewaele, T. Kiss, G. Micera, *Journal of the Chemical Society, Dalton Transactions* (1995) 425-430.
- [66] P. Nunes, I. Correia, I. Cavaco, F. Marques, T. Pinheiro, F. Avecilla, J. Costa Pessoa, *J. Inorg. Biochem.* 217 (2021) 111350.
- [67] J. Costa Pessoa, I. Correia, *Inorganics* 9 (2021) 17.